

K

AN INVESTIGATION ON WAVE FUNCTIONS OF sd-SHELL NUCLEI

1118-01-32-0



AN INVESTIGATION ON WAVE FUNCTIONS OF sd-SHELL NUCLEI - G.A. TIMMER - 1976

G.A. TIMMER

AN INVESTIGATION ON WAVE FUNCTIONS
OF
sd-SHELL NUCLEI

G. A. TIMMER
PASCALSTRAAT 1, AMERSFOORT

**Receptie na afloop van de promotie in het academiegebouw
Domplein 29, Utrecht.**

Stellingen behorende bij het proefschrift

AN INVESTIGATION ON WAVE FUNCTIONS OF sd-SHELL NUCLEI

I

De door Hsu ¹⁾ gegeven bovengrenzen van gereduceerde electromagnetische overgangsterktes binnen een gegeven configuratieruimte kunnen in het geval van $\Delta(J^\pi, T) = 0$ overgangen als volgt scherper worden gesteld. Laat de eigenwaarden en eigenvectoren van de overgangsoperator binnen de N-dimensionale configuratieruimte gegeven zijn door ϵ_i en \vec{v}_i waarbij geldt $\epsilon_1 \leq \dots \leq \epsilon_N$. De sterkst mogelijke overgang vindt plaats tussen toestanden gegeven door $\frac{1}{\sqrt{2}}(\vec{v}_1 + \vec{v}_N)$ en $\frac{1}{\sqrt{2}}(\vec{v}_1 - \vec{v}_N)$ met als overgangsterkte $\frac{1}{4}(\epsilon_1 - \epsilon_N)^2$. De door Hsu opgegeven bovengrens komt overeen met $\max(\epsilon_1^2, \epsilon_N^2)$.

1) L.S. Hsu, *Phys. Lett.* 25B (1967) 588.

II

De konsekwenties van de door Meurders ¹⁾ geïntroduceerde techniek om door middel van extra vergelijkingen de parameters in een kleinste-kwadratenaanpassing in de buurt van de beginwaarden te houden, kunnen elegant worden geformuleerd. Men dient daartoe op te merken dat slechts de eigenwaarden en niet de eigenvectoren van de correlatiematrix ²⁾ beïnvloed worden door de toegevoegde vergelijkingen.

1) F. Meurders et al., *Z. Physik A* 176 (1976) 113;

2) W. Chung, *Thesis Michigan State University* 1976.

III

De door Endt en Van der Leun ¹⁾ gevolgde methode om fouten in vertakkingsverhoudingen op te geven is misleidend.

¹⁾ *P.M. Endt en C. van der Leun, Nucl. Phys. A214 (1973) 1.*

IV

De reactie ($^{18}\text{O}, 2p$), in combinatie met lichte neutronrijke trefplaatkernen, biedt een goede mogelijkheid voor het produceren van neutronrijke kernen zoals ^{29}Mg en ^{34}Si .

V

De informatiestroom van het kernfysische onderzoek naar het Internationale Nucleaire Informatie Systeem ¹⁾ (I.N.I.S.) is in Nederland aanzienlijk breder dan die in de omgekeerde richting. Er is in deze situatie geen verbetering te verwachten zolang de door I.N.I.S. uitgegeven documentatie slechts moeizaam bereikbaar is.

¹⁾ *International Atomic Energy Agency te Wenen, I.N.I.S. Atomindex.*

VI

Voor de bestrijding van de luchtverontreiniging is een gelijkmatige beperking van de emissies van koolwaterstoffen en stikstofoxiden weinig effectief om fotochemische smogvorming te voorkomen.

E. Hesstvedt et al., Institute Report series No. 16, April 1976, University of Oslo.

VII

Om een goede voorspelling te verkrijgen voor electromagnetische vervalseigenschappen is het zinvoller eerst van gegeven golf-functies lineaire combinaties te vormen die worden aangepast aan reeds bekende vervalseigenschappen dan direct gebruik te maken van die golf-functies.

Hoofdstuk II van dit proefschrift.

VIII

De verklaring van Salm en Klepper ¹⁾ voor de waargenomen faseverschuiving in een tijdafhankelijke spinprecessiemeting aan ^{19}F geïmplanteerd in Ni is onjuist.

W. Salm en O. Klepper, Phys. Rev. Lett. 37 (1976) 88.

IX

Teneinde nóg meer luisteraars naar klassieke-verzoekplaten-programma's tevreden te kunnen stellen kan de gebruikelijke procedure om van meerdelige composities slechts één deel ten gehore te brengen worden verfijnd door het toerental van de afspeelapparatuur iets op te voeren en oninteressante passages binnen dat ene deel te verwijderen.

AN INVESTIGATION ON WAVE FUNCTIONS
OF
sd-SHELL NUCLEI

PROEFSCHRIFT

TER VERKRIJGING VAN DE GRAAD VAN DOCTOR IN
DE WISKUNDE EN NATUURWETENSCHAPPEN AAN DE
RIJKSUNIVERSITEIT TE UTRECHT, OP GEZAG VAN
DE RECTOR MAGNIFICUS PROF. DR. A. VERHOEFF,
VOLGENS BESLUIT VAN HET COLLEGE VAN DECANEN
IN HET OPENBAAR TE VERDEDIGEN OP WOENSDAG
20 OKTOBER 1976 DES NAMIDDAGS TE 2.45 UUR

door

GEORGE ALEXANDER TIMMER
GEBOREN OP 14 MAART 1943
TE ROTTERDAM

PROMOTOREN: DR. P.J. BRUSSAARD

DR. P.W.M. GLAUDEMANS

AAN WILLEKE

AAN HANS, LENIE EN NIENKE

AAN MIJN GROOTOUDERS

Tekeningen : Hilde Elberse
Foto's : J.P. Hogeweg
Druk : Elinkwijk b.v. Utrecht

Voorwoord

*Het proefschrift dat U hier nu ziet
een geschrift vol met vreemde verhalen
werd nooit tot dat wat het is
zonder hulp, mijn dank vele malen.*

*Waarde Brussaard, promotor, collega,
Uw scherpe blik dient vermeld
bij het kritisch supervideren
over dat wat hierin wordt verteld.*

*En Glaudemans, d'andere promotor,
zijn visie is het geweest
die het schillenmodel weer deed groeien
langs de lijnen der Utrechtse geest.*

*Ferry Meurders, hij was degene
die vaart in 't werk heeft gebracht;
Ferry, jouw steun kan dan ook
niet hoog genoeg worden geacht.*

*Noem mij de zin ener thesis
zonder toets aan het experiment
toch zou me dat zwaar zijn gevallen
zonder d'inzet en kennis van Endt.*

*Jan van Hienen en ook Henk de Vries
jullie hulp was van zeer grote waarde;
het was toch gedrieën dat wij
onze rekenkennis vergaarden.*

De zorg voor 't boekje zelf
ze typten het zij aan zij;
dank gaat uit naar Sheila McNab,
naar Diet Bos en Monique de la Bey.

Hilde Elberse, de tekenares
der figuren die 't proefschrift verluchten
via Hogeweg droeg zij zo bij
tot 't aanzien van mijn pennevruchten.

Vele anderen dan de genoemden
droegen bij tot een prettige sfeer,
Sjaan van Boggelen is zeker degene
die strijkt met een deel dezer eer.

Het was in dienst van de F.O.M.
dat ik werkte aan wat hier is beschreven,
ik ben dan ook dankbaar dat zij
mij de kans daartoe hebben gegeven.

CONTENTS

INTRODUCTION AND SUMMARY	1
CHAPTER I. A QUANTITATIVE EVALUATION OF THE RELIABILITY OF CALCULATED DECAY PROPERTIES OF NUCLEI IN THE MASS REGION $A = 24 - 28$	3
1. Introduction	3
2. Reliability of calculated transition matrix elements	6
3. Effective single-particle matrix elements	17
3.1. The least-squares fitting procedure	17
3.1.1. The experimental data used in the fitting procedure	18
3.2. E2 transitions and quadrupole moments	19
3.2.1. The results of fit I	22
3.2.2. The results of fit II	23
3.2.3. Discussion of the E2 results	24
3.3. M1 transitions and dipole moments	32
3.3.1. Effective M1 single-particle matrix elements	32
3.3.2. Discussion of the M1 results	32
4. Gamma decay schemes	38
4.1. Assignments of errors to quantities depending on several matrix elements	38
4.2. Results	39
4.2.1. Lifetimes	40
4.2.2. E2/M1 mixing ratios	42
4.2.3. Branching ratios	48
5. Predictions for static moments	54
5.1. Magnetic dipole moments	54
5.2. Electric quadrupole moments	54
6. Allowed beta decay	57
7. Conclusions	61
References	63
CHAPTER II. THE USE OF GAMMA DECAY PROPERTIES FOR THE CONSTRUCTION OF A PHENOMENOLOGICAL HAMILTONIAN	64
1. Introduction	64
2. The construction of wave functions	66
2.1. Restrictions on $a_{\alpha\beta}$	67
2.2. The search procedure for $a_{\alpha\beta}$	68
2.3. The quantity $Q(a_{\alpha\beta})$	70
2.4. Some results	73

3. Construction of a Hamiltonian	74
4. Discussion	77
References	80
CHAPTER III. CALCULATIONS OF SPURIOUS ADMIXTURES IN SHELL-MODEL WAVE FUNCTIONS	
1. Introduction	81
2. Other methods	82
3. The matrix elements of R^2	84
4. Spurious content of shell-model states	89
References	93
SAMENVATTING	94
CURRICULUM VITAE	96

INTRODUCTION AND SUMMARY

In the past two decades a large number of nuclear shell-model calculations have been performed. Some general trends emerge when one follows the historical development of these calculations in Utrecht and elsewhere. In the first place, with the advent of large computers, one sees a steady growth in the size of configuration spaces used for the description of nuclear properties. A second development that can be discerned is a shift of the emphasis that was focussed initially on the proper reproduction of energy spectra towards a proper description of other nuclear properties as well. At least for the sd-shell nuclei ($A = 17-40$), one can observe that the point has been reached where a reasonable description of the energy spectra is taken for granted, at least for low-spin states, and hence the reproduction of the energies is considered to be of decreasing importance for the evaluation of the success of a given calculation. An important stimulus for considering properties other than energy spectra alone, is to be found in the very rapidly growing body of reliable experimental data on gamma-decay properties, spectroscopic factors and static moments.

The work presented in this thesis is partly an extension of calculations described in [1]. Two Hamiltonians were obtained in [1], i.e. the modified surface-delta interaction (MSDI) and the adjusted surface-delta interaction (ASDI).

In the first chapter the results are presented of a calculation of electromagnetic properties with the MSDI and ASDI wave functions. It is concluded that ASDI yields better results than MSDI. In order to describe the sensitivity of the

calculated gamma-decay properties on the Hamiltonian, we introduce in chapter I the concept of a theoretical error to be assigned to these gamma-decay properties. It is found that these errors account reasonably well for the deviations between experiment and theory. It is concluded that in many cases a Hamiltonian may be found which indeed improves this agreement.

In the second chapter the problem of finding such a Hamiltonian is considered. There we obtain wave functions showing a striking agreement for the decay properties. These wave functions differ only slightly from the ASDI wave functions. Then there follows a discussion of ways of constructing a Hamiltonian that yields these wave functions as eigenfunctions with the proper energy. The success of this last step is limited, although some encouraging results were obtained.

The last chapter concerns a problem that is hardly linked with the topics discussed in the first two chapters, i.e. the spurious state problem. This problem, in its generality, arises if a symmetry property of the Hamiltonian is violated. Thus in current shell-model techniques the translational invariance is not properly taken into account. Although we cannot cure this deficiency, the formulae presented give a means of estimating quantitatively the spurious content of shell-model wave functions. The method is applied to some wave functions describing negative parity states in $A = 32$.

Reference

- 1) F. Meurders, P.W.M. Glaudemans, J.F.A. van Hienen and G.A. Timmer, Z. Physik A276 (1976) 113.

CHAPTER I

A QUANTITATIVE EVALUATION OF THE RELIABILITY OF CALCULATED DECAY PROPERTIES OF NUCLEI IN THE MASS REGION $A = 24 - 28$

G.A. TIMMER, F. MEURDERS, P.J. BRUSSAARD

and

J.F.A. van HIENEN[†]

Abstract: Electromagnetic transition rates and log ft values were calculated for transitions between positive-parity states in the $A = 24 - 28$ mass region. The wave functions used were taken from a previous paper. In general we found satisfactory agreement with experiment. In order to have a measure of the stability of the results against changes in the Hamiltonian a method was developed for assigning errors to calculated transition properties. The re-normalized single-particle matrix elements of the E2 and M1 transition operators were determined in a phenomenological way. To this end use was made of the errors just mentioned. It was found that good agreement was obtained with bare-nucleon M1 single-particle matrix elements and a state independent effective isoscalar charge for the E2 operator. Predictions for static moments are given.

1. Introduction

In a shell-model calculation with a phenomenological effective interaction fitted to a number of experimental data, it is not immediately evident how well determined the interaction and hence the calculated wave functions are. The dynamical properties (e.g. electromagnetic transition

[†] Present address: Cyclotron Laboratory, M.S.U., East Lansing, Michigan, 48823, U.S.A.

rates) calculated with these wave functions may sometimes deviate appreciably from the experimental data, even if one uses effective transition operators. It would be quite useful to know then whether the discrepancies could be ascribed to deficiencies of the Hamiltonian. It will be shown that some calculated observables are often very sensitive to a slight change in the Hamiltonian while others are not.

In this paper the calculations of decay properties of positive-parity states in the mass region $A = 24 - 28$ are described. They represent a continuation of earlier shell-model calculations [1].

In [1] two different effective interactions were considered in a truncated $1s-0d$ shell-model configuration space. The first of these interactions, the modified surface-delta interaction (MSDI), see [2], served as a starting point for the generation of the second interaction which is referred to as the adjusted surface delta interaction (ASDI). Subsequently, we considered two observables, viz. energies and spectroscopic factors for single-particle transfer.

Here we present calculations of E2 and M1 decay rates using the MSDI and the ASDI wave functions. We shall confirm the conclusion drawn in [1], namely that the ASDI wave functions constitute an improvement over the MSDI wave functions.

In section 2 a detailed account will be given of a method of assigning errors to calculated transition matrix elements. These errors are intended to give a measure for the stability of such matrix elements when the Hamiltonian is changed. In this way we may obtain an impression of the reliability of calculated transition matrix elements. The method of assigning

errors is based on the observation that an improvement in the reproduction of the energies often leads to an improvement in the other observables as well. The outline of the error assignment procedure given in [3] is superseded by the present paper.

A truncation of the configuration space, unavoidable for practical calculations, gives rise to renormalization effects. Many attempts based on perturbational techniques have been made to obtain a renormalized Hamiltonian and renormalized transition operators. Owing to the poor convergence [4] of the perturbation expansions, these attempts have not led so far to quantitatively satisfying results. We therefore adopt a phenomenological approach to obtain the renormalized transition operators. To this end we consider in the first part of section 3 different ways of parametrizing the E2 and M1 operators. The relevant parameters will be fitted to the experimental data. The results of section 2 are essential when weighting factors are introduced into the fitting procedure. Another point stressed in the first part of section 3 is the dependence of the fitted parameters on the set of experimental data which have been taken into account. In our opinion this dependence deserves more attention than it has received hitherto in the literature dealing with phenomenological Hamiltonians. The remainder of section 3 is devoted to a comparison of calculated and experimental E2 and M1 transition rates and static moments.

We present not only electric and magnetic reduced transition strengths and moments but we also deal with quantities derived from them like lifetimes, E2/M1 mixing ratios and branching ratios.

We do this mainly because of a rather trivial extension of the error assignment procedure. This extension leads to the observation that quite often the quantities mentioned above are less sensitive to details of the Hamiltonian than the separate transition matrix elements.

In some cases we consider explicit changes of the wave functions without specifying the underlying changes of the Hamiltonian. Unitary transformations among the given wave functions are constructed in such a way that the best possible agreement with experiment is obtained. In section 4 we discuss some remarkable results of this procedure. A more systematic investigation along these lines is under consideration at present.

In the last two sections we present some calculations with the ASDI wave functions that are somewhat detached from the main lines of this paper. Section 5 is devoted to predictions for static moments, and in section 6 allowed β -decay is treated.

2. Reliability of calculated transition matrix elements.

In a shell-model calculation generating wave functions for the evaluation of electromagnetic transition rates and log ft values one needs the appropriate effective interaction for the model space chosen. The various methods used to determine this interaction do not produce identical results.

In a previous paper [1] we considered two effective interactions and calculated energies and spectroscopic factors for the mass region under consideration, viz. $A = 24-28$.

The first of these interactions, the modified surface-delta interaction (MSDI), contains four parameters that must be adjusted to experimental energies. These four parameters determine all 63 two-body matrix elements of the interaction in the sd shell-model space. It was possible to improve the agreement of the calculated energies with the experimental values when subsequently small variations of the two-body matrix elements with respect to their MSDI values were allowed. The resulting effective interaction is called the adjusted surface delta interaction (ASDI).

It was found that on improving the agreement between the experimental and the calculated energies the results obtained for spectroscopic factors were also of better quality. In section 3 it will be shown that the same applies to M1 and E2 transition rates. In view of these facts one would like to quote an error for the calculated nuclear properties as a measure of the uncertainties in the Hamiltonian. The magnitude of this error will then be related to the agreement for the energies.

To achieve this we shall first give a simple expression for the change of calculated transition matrix elements (CTME), resulting from small changes of the Hamiltonian, in terms of first-order perturbation theory.

The eigenvalue equation of the effective Hamiltonian reads:

$$H|K,m\rangle = E_m^K |K,m\rangle, \quad (2.1)$$

where the abbreviation $K \equiv (J^\pi, T)$ is introduced and the symbol $m (m = 1, 2, \dots)$ stands for the eigenvector number within the set of eigenstates labelled by K , so that $E_{m+1}^K > E_m^K$.

A small change δH of the Hamiltonian H will cause changes $\delta \langle K, m | 0 | K', m' \rangle$ in the matrix elements of a transition operator O . Applying first-order perturbation theory to the initial and final states one obtains the relation:

$$\delta \langle K, m | 0 | K', m' \rangle = \sum_{i \neq m} \frac{\langle K, m | \delta H | K, i \rangle \langle K, i | 0 | K', m' \rangle}{E_m^K - E_i^K} + \sum_{i' \neq m'} \frac{\langle K, m | 0 | K', i' \rangle \langle K', i' | \delta H | K', m' \rangle}{E_{m'}^{K'} - E_{i'}^{K'}} \quad (2.2)$$

The problem of degeneracy can be ignored for the Hamiltonians considered, viz. MSDI and ASDI.

The variation δH should now be specified. Let H' represent the (unknown) Hamiltonian that yields the best agreement with experiment in the chosen configuration space. Then δH is defined by the relation $\delta H = H' - H$. The main assumption we shall make about H' is that the deviations of its eigenvalues from the experimental (Coulomb corrected) energies are small compared with the level spacings. The diagonal matrix elements of δH are then given by:

$$\langle K, m | \delta H | K, m \rangle = E_{m \text{ exp}}^K - E_m^K, \quad (2.3)$$

where $E_{m \text{ exp}}^K$ represents the experimental energy of the state $|K, m\rangle$. Thus these diagonal matrix elements can be extracted from the experimental data.

The off-diagonal matrix elements of δH in eq. (2.2) cannot be determined from the experimental data. Let Q_{mi}^K be an esti-

mate of the matrix element $\langle K,m|\delta H|K,i\rangle$. We shall now make the assumption that the off-diagonal matrix elements of δH can be treated as uncorrelated variables. Then an estimate $\Delta_{mm'}$, for the change in $\langle K,m|0|K',m'\rangle$ under the influence of δH is given by:

$$\Delta_{mm'} = \left[\sum_{i \neq m} \left\{ \frac{\langle K,i|0|K',m'\rangle}{E_m^K - E_i^m} Q_{mi}^K \right\}^2 + \sum_{i' \neq m'} \left\{ \frac{\langle K,m|0|K',i'\rangle}{E_{m'}^{K'} - E_{i'}^{K'}} Q_{m'i'}^{K'} \right\}^2 \right]^{1/2} \quad (2.4)$$

In the remainder of this paper we shall refer to this quantity as the theoretical error in $\langle K,m|0|K',m'\rangle$. Since the indices i and i' run over eigenstates of the model Hamiltonian H , this error will not account for deficiencies in the configuration space. We shall comment on this point at the end of this section.

Equation (2.4) needs some modification when $K = K'$ holds. Then the terms $i = m'$ and $i' = m$ in eq. (2.2) must first be taken together before the incoherent quadratic sum is formed, since they involve the same matrix element of δH and hence may not be considered as independent.

The summations in eq. (2.4) will now be divided into two parts. The first part includes the summation over the intermediate states of which the eigenvector number i or i' is near m or m' , respectively. In the applications we have $m, m' \leq 2$ and we limit the terms in the first part to $i, i' \leq 4$. The second part contains the remaining terms.

Let us now consider the first part. In order to obtain an estimate for Q_{mi}^K of the off-diagonal matrix element of δH to be used in this part of the summation, we make the following ansatz:

$$Q_{mi}^K = \frac{1}{2} \left\{ |E_m^K - E_{m \text{ exp}}^K| + |E_i^K - E_{i \text{ exp}}^K| \right\}. \quad (2.5)$$

Thus we replace each off-diagonal matrix element of δH by the arithmetic mean of the corresponding two diagonal matrix elements. In some cases the necessary experimental information, i.e. $E_{i \text{ exp}}^K$, was lacking even for low values of i . In such cases an average value over the available states K is taken:

$$D_i \equiv |E_{i \text{ exp}} - E_i| = \sum_{K'} |E_{i \text{ exp}}^{K'} - E_i^{K'}| / \sum_{K'} 1, \quad (2.6)$$

where the summation over K' is restricted to those combinations for which $E_{i \text{ exp}}^{K'}$ is known. In this way we introduce an eigenvector number dependent measure of the expected deviation between experimental and calculated energies. In table 2.1 we show the result of this manipulation for the MSDI and ASDI Hamiltonians.

This ansatz (2.5) of course cannot be justified rigorously; it exhibits, however, the following desirable features. (i) If the energy of a state $|K, m\rangle$ is poorly reproduced by H , we expect $|K, m\rangle$ to mix more easily with other states like $|K, i\rangle$ under the influence of δH than in a case where the energy was calculated accurately. (ii) The hermiticity of δH is retained, i.e. $Q_{mi}^K = Q_{im}^K$. The appropriateness of the ansatz (2.5) is demonstrated by the results of the present

Table 2.1

The average difference (in MeV) between calculated and experimental energies as a function of the eigenvector number m

m :	1	2	3	4
MSDI	0.1	0.3	0.6	0.6
ASDI	0.1	0.2	0.4	0.6

calculations. In most cases a definite correlation is obtained between the size of the errors one thus assigns to the CTME and the quality of the agreement between the theoretical and the experimental values.

We now turn to the second part of the summation in eq. (2.4), i.e. $i, i' > 4$, again considering only the cases $m, m' \leq 2$. These terms are neglected. Although we thus disregard the majority of the terms in eq. (2.4) this omission can be made plausible numerically in the following way. After a complete diagonalization of the ASDI Hamiltonian for all K considered, the matrix elements of the operator O in eq. (2.4) are calculated. Subsequently the following quantity is evaluated (cf. eq. (2.4)):

$$Q_{mm'} = |\langle K, m | 0 | K', m' \rangle| \left[\sum_{i>4} \left\{ \frac{\langle K, i | 0 | K', m' \rangle}{E_m^K - E_i^K} \right\}^2 + \sum_{i'>4} \left\{ \frac{\langle K, m | 0 | K', m' \rangle}{E_{m'}^{K'} - E_{i'}^{K'}} \right\}^2 \right]^{-\frac{1}{2}} \quad (2.7)$$

If $Q_{mm'}$ turns out to be much larger than an estimate for a typical value of Q_{mi}^K with $i > 4$ and $m \leq 2$, we may conclude that the omission of the second part of the summation in eq. (2.4) is justified. For $m \leq 2$ the energies are reproduced within 0.2 MeV (see table 2.); we assume that a typical off-diagonal matrix element of δH between states $m \leq 2$ and high-lying states $i > 4$ should be considerably smaller than this value. Thus if $Q_{mm'}$ has a magnitude $\lesssim 0.2$ MeV serious doubt must be cast upon the legitimacy of our assumption that we may neglect the second part in the summations in eq. (2.4). We shall now discuss the results of the numerical evaluation of $Q_{mm'}$.

Although the calculated values of $Q_{mm'}$ showed large variations, the following trends appeared.

- i) $Q_{mm'}$ is generally larger for E2 transitions than for M1 transitions.
- ii) For transitions between yrast levels Q_{11} is large, typically $\gtrsim 5$ MeV for E2 transitions and $\gtrsim 2$ MeV for M1 transitions.

- iii) For transitions involving one non-yrast level Q_{mm} , is of the order of 0.5 MeV for E2 transitions and 0.2 MeV for M1 transitions. Especially in this case large variations occur.
- iv) For transitions between two non-yrast levels the value of Q_{mm} , is generally found to be so small that our assumption that we may neglect the summations over high-lying intermediate states seems not to be justified. There are, however, very few such transitions that can be compared with experiment. A notable exception is provided by the static moments of non-yrast levels. For both the electric quadrupole moments and the magnetic dipole moments it was found that Q_{mm} tends to be very large. Here we have a special case of the situation described in eq. (2.8) which will be discussed below.

After discarding the summations over higher intermediate states in eq. (2.4) we are now in a position to investigate the reliability of the error assignment procedure.

The ASDI results displayed in tables 3.1 and 3.2 are illustrated in fig. 2.1. The relative difference between the calculated E2 matrix elements and the experimental data, $(|M_c| - |M_e|)/|M_e|$, is plotted *versus* the ratio of the total error and the calculated matrix element $|M_c|$. The total error is obtained by adding the theoretical and experimental errors quadratically. In line with the discussion following eq. (2.7), the non-yrast to non-yrast transitions are not taken into account. The $5/2_2^+ \rightarrow 1/2_1^+$ transition in ^{25}Al has been omitted since we have serious doubts about the reliability of the experimental strength quoted. The two curves repre-

sent the cases for which the experimental matrix element is given by either of the relations $|M_e| = |M_c| \pm \sqrt{(\Delta M_c)^2 + (\Delta M_e)^2}$. In the region between the two curves the difference between experiment and theory is smaller than the total error.

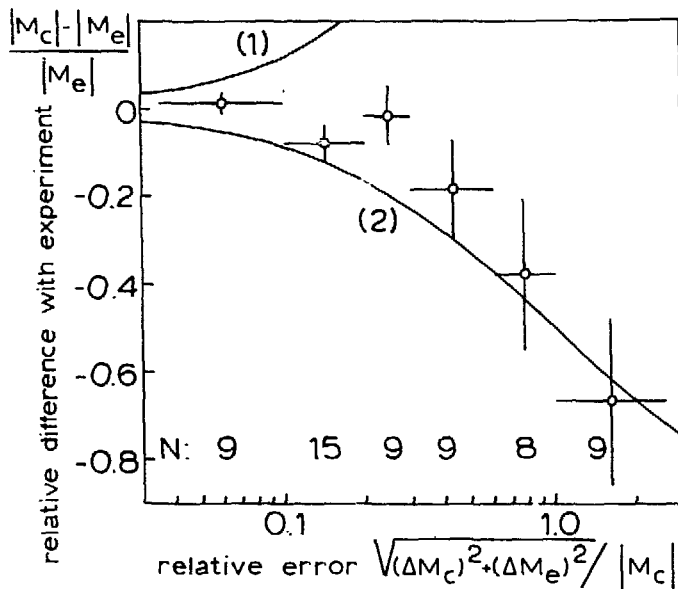


Fig. 2.1. The difference between the experimental and calculated E2 matrix elements (see tables 3.1 and 3.2) as a function of the ratio of the total error and the calculated E2 matrix element. The average value and the standard deviation are given for a number of intervals of the abscissa. The length of each interval is indicated by the horizontal bar; N is the number of cases in each interval.

We shall now discuss some aspects of the error assignment procedure that have been ignored so far. First we shall mention a tricky point that may arise when the quantity $|E_{m_{\text{exp}}}^K - E_m^K|$ is evaluated for the ansatz (2.5).

Then one takes the energy difference between the m-th experimental eigenstate with spin K and the m-th calculated eigenstate with the same spin. The underlying assumption is that when δH is switched on the eigenstate $|K, m\rangle$ of H will converge to the m-th eigenstate of H' , with H' defined as before. We encountered one case where this assumption proved to be incorrect, viz. the 2_2^+ and the 2_3^+ states in ^{28}Si . This case will be discussed in detail in section 4.

A second remark concerns the class of very large CTME. This class contains many of the E2 matrix elements between yrast levels and many of the E2 and M1 static moments. We call a matrix element $\langle K, m | O | K', m' \rangle$ large if the following approximate relations are satisfied:

$$\sum_i |K, i\rangle \langle K, i | O | K', m' \rangle \approx |K, m\rangle \langle K, m | O | K', m' \rangle ,$$

$$\sum_{i'} \langle K, m | O | K', i' \rangle \langle K', i' | \approx \langle K, m | O | K', m' \rangle \langle K', m' | . \quad (2.8)$$

This means that for a given initial state $|K', m'\rangle$ the total strength of the operator O to states with given spin K is concentrated mainly in one state, i.e. $|K, m\rangle$, and vice versa. If these relations (2.8) are substituted into eq. (2.2) one finds that $\langle K, m | O | K', m' \rangle$ is very insensitive to the choice of the Hamiltonian. In such cases the higher-order terms in δH should be taken into account. In view of the tentative character of the error assignment procedure this point was not considered further. Moreover, as is clear from fig. 2.1, it is found that the agreement between theory and experiment is about as good as may be expected for these cases, i.e.

$$\Delta M_c \ll |M_c| .$$

The same remarks about the omission of higher-order terms in δH apply to cases where one calculates very large errors.

In section 4 we shall give a trivial extension of the error assignment procedure to quantities that depend on more than one CTME such as mixing ratios etc.

We shall now discuss an application of these theoretical errors. The errors are intended to give some measure of the possible change in a CTME in case a better Hamiltonian is required. An improper choice of the Hamiltonian is, however, not the only source of errors in CTME. There are two other deficiencies, viz. an improper choice of the configuration space (it may be too heavily truncated) and an inappropriate renormalization of the operator considered. If we arrive at a completely wrong result with a small error assigned to it we must conclude that one of these deficiencies occurs. It should be mentioned that there is one class of transition matrix elements where the conclusion about the deficiencies of the configuration space can be drawn regardless of the choice of the Hamiltonian. Since for a finite model space the transition operators are bounded, an upper limit exists for the transition strength which is independent of the Hamiltonian; for further details see [5]. The few relevant cases we encountered will be considered explicitly in the next section.

3. Effective single-particle matrix elements

Besides the errors in the wave functions described in the previous section there are uncertainties in the single-particle transition operators used in the truncated configuration space. The effects of the truncation of the configuration space can be compensated for to a large extent by a renormalization procedure. There are two approaches possible to achieve this renormalization. One method is to parametrize the operators in some way and adjust them to the experimental data. The other way is to use perturbation theory to calculate the corrections required because part of the configuration space is ignored. Here we shall follow the former, phenomenological approach. As the electromagnetic transition operators are single-particle operators, all matrix elements between many-particle states can be expressed linearly in terms of matrix elements between single-particle states. The single-particle matrix elements (SPME) can now be considered as adjustable parameters in a least-squares fitting procedure.

3.1. THE LEAST-SQUARES FITTING PROCEDURE

The principles of the least-squares fitting procedure used are given in [6]. However, the procedure we followed differs from the one referred to in two respects.

- i) The experimental data do not determine the sign of the experimental transition matrix element (ETME), but determine only the absolute value. Exceptions are of course the static moments. In [6] the sign of an ETME

- is equated to the sign of the CTME that results if the bare-nucleon single-particle matrix elements are used. A CTME resulting from a calculation with the fitted single-particle matrix elements may have a different sign. When this was the case we repeated the fitting procedure with the sign of the ETME reversed as well.
- ii) We took the weighting factors of the linear equations to be inversely proportional to the quadratically added experimental and theoretical errors. Thus our weighting factors show no explicit dependence on the magnitude of the matrix elements or on the eigenvector numbers of the states involved. In view of the results of the evaluation of eq. (2.7), discussed in section 2, it was decided to fit only those matrix elements $\langle K, m | 0 | K', m' \rangle$ where $m + m' \leq 3$ holds.

Some problems of self-consistence now arise. The theoretical errors that affect the weighting factors depend on the quantities to be fitted, viz. the single-particle matrix elements. In fact an iterative scheme has to be followed. The first step is to make an initial guess for the SPME to determine theoretical errors. The second step is to use the errors in the weighting factors of the equations to determine new SPME. This procedure is repeated until convergence occurs.

3.1.1. The experimental data used in the fitting procedures
The experimental data used to fit the SPME were taken from [7,8]. These references contain those experimentally known E2 and M1 transition strengths the experimental errors of which are not larger than 50 %. The static moments were derived from [9]. In some cases we used more recent values which

will be referred to explicitly. Neither the transitions involving high-spin states ($J \gtrsim 6$) nor transitions in neutron rich nuclei ($T > 3/2$) were fitted since the necessary wave functions were not available.

A point that should be considered is the dependence of the results of the fitting procedures on the selection of the experimental data. To investigate this dependence we performed the fits for different sub-sets of the data available. Each sub-set was labelled by the minimal experimental strengths, S_{\min} , which was taken into account. If the fitted value of a parameter is strongly dependent on S_{\min} , then we must conclude that the way that was chosen to parametrize the transition operator is not meaningful.

3.2. E2 TRANSITIONS AND QUADRUPOLE MOMENTS

In the second-quantization formalism the E2 transition operator is given as:

$$O(E2) = \sum_{a,b,T} e_{ab}^T (-1)^T \frac{\langle a ||| E2^T ||| b \rangle}{\sqrt{5(2T+1)}} \left[\eta_a^+ \times \tilde{\eta}_b \right]^{2,T} \quad (3.1)$$

Here the summation extends over the single-particle states a and b and over the isoscalar and isovector parts, $T = 0$ and $T = 1$. The fermion creation operator

$$\eta_a^+ \equiv \eta_{j_a, m_a, \frac{1}{2}, \tau_a}^+ \quad \text{and the time-reversed destruction}$$

$$\text{operator } \tilde{\eta}_b \equiv \tilde{\eta}_{j_b, m_b, \frac{1}{2}, \tau_b} = (-1)^{j_b + m_b + \frac{1}{2} + \tau_b} \eta_{j_b, -m_b, \frac{1}{2}, -\tau_b}$$

are coupled to the proper multipolarities in configuration space and in isospin space. The reduced bare-nucleon SPME $\langle a ||| E2^T ||| b \rangle$ are multiplied by state-dependent effective charges e_{ab}^T to account for the renormalization of the E2 operator in the truncated configuration space.

The matrix element $\langle a ||| E2^T ||| b \rangle$ was calculated with harmonic oscillator wave functions. The radial matrix elements were calculated with the size parameter $b = (\hbar/m\omega)^{1/2}$ that was determined from the well-known empirical relation $\hbar\omega = 41A^{-1/3}$ MeV. It should be noted that effective charges need not represent merely the renormalization effects. They could be interpreted as alterations of the radial matrix elements, since the latter always occur multiplied with e_{ab}^T . A discussion about whether this re-interpretation is justified is beyond the scope of this paper.

A procedure often followed is to take a state-independent isoscalar charge e^0 and to use for the isovector part of the E2 operator the bare-nucleon matrix elements, i.e. $e_{ab}^1 = +e$ for all a and b, which thus leaves one free parameter. We shall refer to this procedure as fit I.

In view of the large amount of experimental data available in the mass region under consideration it might seem worthwhile attempting a calculation without making this restriction. Then for an sd-shell calculation one would deal with a set of ten free parameters. However, there appeared to be little point in considering the state-dependence of the effective charge in its full generality. There are two reasons for not considering the isovector charges as adjustable parameters, i) Out of the 59 E2 matrix elements that could be included in the fitting procedure, 19 are between

$T = 0$ states, which thus determine e_{ab}^0 only. ii) The result of the fit for the remaining cases is quite insensitive to the choice of e_{ab}^1 , since most CTME for both the MSDI and the ASDI case were determined largely by the isoscalar contribution. The latter phenomenon is demonstrated in fig. 3.1. In these histograms we plotted the frequency with which a certain ratio between the bare-nucleon isovector and isoscalar matrix elements occurs within the set of E2 matrix elements that could be fitted. Corresponding transitions between pairs of analogue states are counted once.

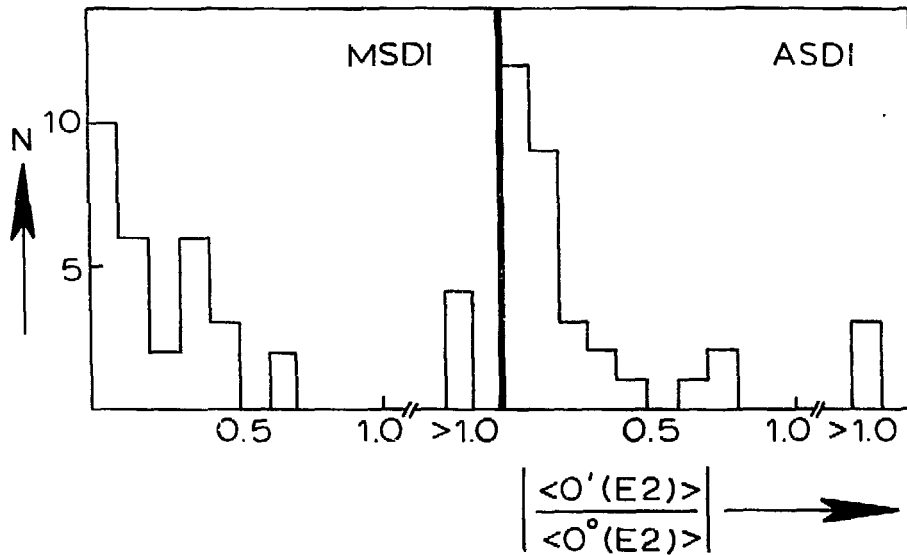


Fig. 3.1. The number of cases N as a function of the absolute ratio between the isovector and isoscalar parts of the E2 matrix elements.

Two fits were actually considered, viz. the fit previously called fit I with a state-independent effective charge as a free parameter, and a fit, to be referred to as fit II, where the state-dependent effective isoscalar charges were allowed to vary independently.

3.2.1. *The results of fit I.* The procedure described at the end of section 3.1 led after one iteration to effective isoscalar charges $e^0 = 2.33e$ and $e^0 = 2.15e$ for the MSDI and the ASDI case, respectively. With these values entering into the theoretical errors we performed the fit for a number of sub-sets of the experimental data. The results are displayed in fig. 3.2. The error bars in this picture are the statistical errors in the parameter e^0 ; they result from the fitting procedure.

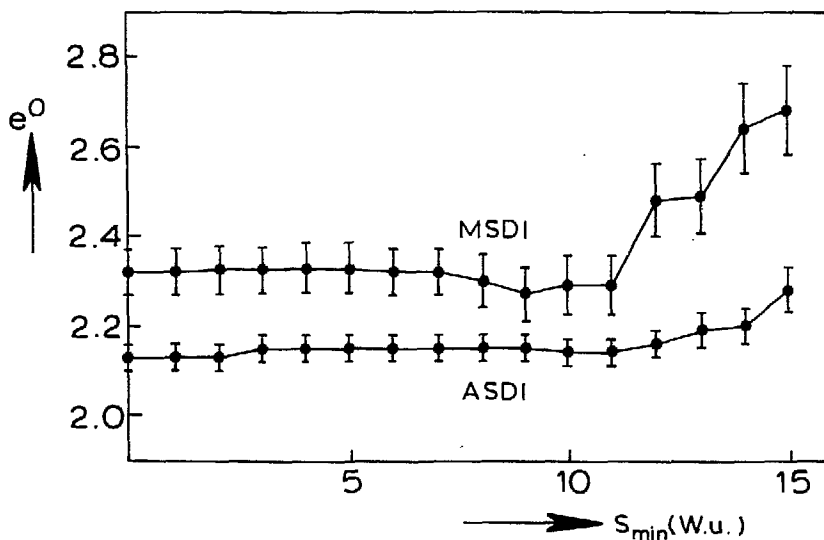


Fig. 3.2. The isoscalar effective charge $e^0 = e_p + e_n$ as a function of the minimal experimental strength S_{\min} used in the fit.

Although there is a tendency for the large matrix elements to require a larger effective charge we may conclude, especially for the ASDI, that a state-independent effective isoscalar charge is a meaningful quantity in the sense described in section 3.1.2. It should be mentioned in this connection that, especially for the MSDI, a different way of calculating weighting factors (i.e. according to [6]) gives a completely different value of e^0 for small values of S_{\min} .

The results for individual transitions obtained with fit I will be discussed in section 3.2.3.

3.2.2. *The results of fit II.* Although for fit II we have a larger set of adjustable parameters at our disposal than for fit I, there resulted no noticeable improvement. This can be understood in the following way. In the first place it proved impossible to fit the effective charges involving the $d_{3/2}$ state in a reliable way. The $d_{3/2}$ content of the MSDI and the ASDI wave functions was not large enough. The total isoscalar transition matrix elements are thus mainly determined by the $d_{5/2} \rightarrow d_{5/2}$ and the $s_{1/2} \rightarrow d_{5/2}$ transition amplitudes. It turns out that for the majority of the CTME considered the interference between these amplitudes is constructive, which reduces the relative importance of the $d_{3/2}$ amplitudes even further. The effective charges that involve the $d_{3/2}$ state were kept constant at a value $e_{ab}^0 = 2e$ for the remainder of the procedure. The behaviour of the two remaining parameters, viz, $e_{d_{5/2}d_{5/2}}^0$ and $e_{s_{1/2}d_{5/2}}^0$, as a function of the minimal strength that was fitted, is shown in fig. 3.3.

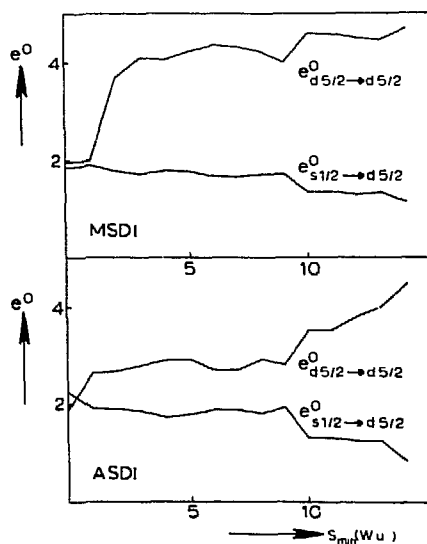


Fig. 3.3. The state-dependent isoscalar effective charges as a function of the minimal experimental strength S_{\min} used in the fit.

Thus, in view of the strong dependence on S_{\min} , this way of parametrizing the operator seems not to be justified.

When one combines i) the afore-mentioned constructive interference between the $d_{5/2} \rightarrow d_{5/2}$ and $s_{1/2} \rightarrow d_{5/2}$ transition amplitudes and ii) the opposite trends of the respective effective charges, one sees why the state-independent effective charge shows no strong dependence on S_{\min} .

It was decided not to pursue the idea of a state-dependent charge any further.

3.2.3. *Discussion of the E2 results.* The E2 transition strengths presented in table 3.1 and the quadrupole moments in table 3.2 resulted from fit I described in the previous section.

Table 3.1

Comparison between experimental and calculated E2 transition strengths

	Transition				E2 Strength (W.u.)				
	J_i^π, E_{x_i} (MeV)	J_f^π, E_{x_f} (MeV)			MSDI ^{a)}	ASDI ^{b)}	EXP ^{c)}		
²⁴ Mg	2_1^+	1.37	0_1^+	0	19 ± 2	18 ± 1	20 ± 1 ^{d)}		
	4_1^+	4.12	2_1^+	1.37	5 ± 7	21 ± 2	23 ± 4		
	2_2^+	4.24	0_1^+	0	0.8 ± 1.7	0.9 ± 0.4	1.1 ± 0.1		
			2_1^+	1.37	6 ± 4	4 ± 2	2.4 ± 0.3		
	3_1^+	5.24	2_1^+	1.37	1 ± 2	1.7 ± 0.7	2.0 ± 0.3		
	4_2^+	6.01	2_1^+	1.37	19 ± 8	0.2 ± 0.6	1.0 ± 0.2		
			2_2^+	4.24	2 ± 5 ^{e)}	4 ± 9 ^{e)}	9 ± 4		
	0_2^+	6.43	2_1^+	1.37	3 ± 8	≈ 0 ± 0.05	0.24 ± 0.08		
			2_2^+	4.24	13 ± 16 ^{e)}	12 ± 7 ^{e)}	3.5 ± 1.3		
	²⁵ Mg	$1/2_1^+$	0.59	$5/2_1^+$	0	0.6 ± 1.9	0.5 ± 1.3	0.54 ± 0.01	
$3/2_1^+$		0.97	$5/2_1^+$	0	1.7 ± 1.7	0.9 ± 0.7	0.7 ± 0.3 ⁱ⁾		
$7/2_1^+$		1.61	$5/2_1^+$	0	22 ± 4	23 ± 1	35 ± 8 ^{f)}		
$5/2_2^+$		1.96	$5/2_1^+$	0	0.2 ± 1.4	0.2 ± 0.3	0.4 ± 0.2 ^{f)}		
			$1/2_1^+$	0.59	15 ± 2	14 ± 1	18 ± 7 ^{f)}		
$7/2_2^+$		2.74	$5/2_1^+$	0	2 ± 3	≈ 0 ± 0.04	0.16 ± 0.04 ^{f)}		
			$3/2_1^+$	0.97	15 ± 4	15 ± 1	23 ± 3 ^{f)}		
$9/2_2^+$		4.06	$5/2_1^+$	0	≈ 0 ± 1.0	1.1 ± 1.8	1.7 ± 0.3		
	$7/2_1^+$		1.6	8 ± 3	3 ± 4	3.1 ± 1.2			

Table 3.1 (cont.)

		Transition		E2 Strength (W.u.)				
		J_i^π, E_{xi} (MeV)	J_f^π, E_{xf} (MeV)	MSDI ^{a)}	ASDI ^{b)}	EXP ^{c)}		
²⁵ Al	$1/2_1^+$	0.45	$5/2_1^+$	0	3 ± 6	2 ± 3	3.0 ± 0.1	
	$3/2_1^+$	0.95	$5/2_1^+$	0	3 ± 3	2.0 ± 1.3	1.8 ± 0.7	
	$5/2_2^+$	1.79	$1/2_1^+$	0.45	16 ± 3	15 ± 1	31 ± 5 ^{e)}	
$3/2_1^+$			0.95	5 ± 2	5.5 ± 1.0	8.1 ± 1.5		
²⁶ Mg	2_1^+	1.81	0_1^+	0	14 ± 5	14 ± 1	12.6 ± 0.5 ^{d)}	
	2_2^+	2.94	0_1^+	0	1 ± 5	0.2 ± 0.5	1.0 ± 0.3	
			2_1^+	1.81	17 ± 4	11.0 ± 0.5	13 ± 6	
	4_1^+	4.32	2_1^+	1.81	0.2 ± 1.5	9 ± 2	5.8 ± 1.9	
	4_2^+	4.90	2_2^+	1.81	17 ± 9	5 ± 3	9 ± 3	
²⁶ Al	3_1^+	0.42	5_1^+	0	3 ± 2	8 ± 3	7.4 ± 0.2	
	4_1^+	2.07	5_1^+	0	7 ± 4	2.6 ± 1.1	3.1 ± 0.5 ^{g)}	
	3_2^+	2.37	1_1^+	1.06	6 ± 8	7 ± 12	4.7 ± 1.1	
	5_2^+	3.40	5_1^+	0	4 ± 3	0.3 ± 0.4	1.5 ± 0.4	
			3_1^+	0.42	1 ± 6	1.4 ± 1.8	5.8 ± 1.6	
²⁶ Si	2_1^+	1.80	0_1^+	0	15 ± 2	10 ± 2	7 ± 3	
	0_2^+	3.33	2_1^+	1.80	0 ± 3	1 ± 3	8 ± 3	
²⁷ Mg	$3/2_1^+$	0.98	$1/2_1^+$	0	8 ± 3	8.4 ± 0.9	6.3 ± 1.7	
	$5/2_1^+$	1.70	$1/2_1^+$	0	5 ± 5	10 ± 3	9.6 ± 1.6	

Table 3.1 (cont.)

		Transition				E2 Strength (W.u.)		
		J_i^π, E_{xi} (MeV)	J_f^π, E_{xf} (MeV)		MSD1 ^{a)}	ASD1 ^{b)}	EXP ^{c)}	
²⁷ Mg	5/2 ₂ ⁺	1.94	1/2 ₁ ⁺	0	7 ± 5	2 ± 3	1.8 ± 0.3	
²⁷ Al	1/2 ₁ ⁺	0.84	5/2 ₁ ⁺	0	4 ± 3	10 ± 2	8.8 ± 1.0	
	3/2 ₁ ⁺	1.01	5/2 ₁ ⁺	0	14 ± 3	7.7 ± 1.3	9.5 ± 1.7	
	7/2 ₁ ⁺	2.21	5/2 ₁ ⁺	0	18 ± 1	13 ± 1	11 ± 1	
	5/2 ₂ ⁺	2.73	3/2 ₁ ⁺	1.01	5 ± 3	13 ± 2	7 ± 3	
	9/2 ₁ ⁺	3.00	5/2 ₁ ⁺	0	6.4 ± 0.4	6.0 ± 1.0	7.4 ± 0.7	
	11/2 ₁ ⁺	4.51	7/2 ₁ ⁺	2.21	1 ± 5	5 ± 5	6.2 ± 0.6	
			9/2 ₁ ⁺	3.00	1 ± 4	4 ± 4	9.0 ± 1.4 ^{h)}	
		7/2 ₂ ⁺	4.58	5/2 ₁ ⁺	0	0.5 ± 0.6	0.6 ± 0.4	0.18 ± 0.09
	9/2 ₂ ⁺	5.43	5/2 ₁ ⁺	0	0.5 ± 0.4	0.9 ± 1.0	0.41 ± 0.13	
²⁷ Si	1/2 ₁ ⁺	0.78	5/2 ₁ ⁺	0	7 ± 4	15 ± 2	11 ± 1	
	3/2 ₁ ⁺	0.96	5/2 ₁ ⁺	0	13 ± 3	6.4 ± 1.6	7.5 ± 1.8	
	7/2 ₁ ⁺	2.16	5/2 ₁ ⁺	0	14 ± 1	9 ± 1	9 ± 3	
²⁸ Al	0 ₁ ⁺	0.97	2 ₁ ⁺	0.03	1 ± 3	1 ± 3	3.8 ± 0.6	
	1 ₁ ⁺	1.37	3 ₁ ⁺	0	3 ± 10	0.2 ± 0.7	5 ± 1	
	1 ₂ ⁺	1.62	3 ₁ ⁺	0	2 ± 10	7.4 ± 1.8	4.8 ± 1.1	

Table 3.1 (cont.)

		Transition		E2 Strength (W.u.)				
		J_i^π, E_{xi} (MeV)	J_f^π, E_{xf} (MeV)	MSDI ^{a)}		ASDI ^{b)}		EXP ^{c)}
²⁸ Si	2_1^+	1.78	0_1^+ 0	14	± 1	13.0	± 0.2	13.0 ± 1
	4_1^+	4.62	2_1^+ 1.78	19	± 6	17	± 1	14 ± 1
	0_2^+	4.98	2_1^+ 1.78	3	± 5	5.8	± 1.8	11 ± 2
	4_2^+	6.89	2_1^+ 1.78	1	± 5	0.2	± 0.5	0.57 ± 0.09
	2_2^+	7.38	0_1^+ 0	0.8	± 0.9	0.5	± 0.2	0.36 ± 0.09

a) $e^0 = 2.33$ e.

b) $e^0 = 2.15$ e.

c) Experimental data from [7,8]; more recent data taken into account are quoted explicitly.

d) Ref. 11.

e) Not used in the fit; see discussion in the text.

f) Ref. 22.

g) Ref. 23.

h) Ref. 24.

i) Ref. 12.

Table 3.2

Comparison between experimental and calculated quadrupole moments

	J^π	E_x (MeV)	$Q(efm^2)$		
			MSDI ^{a)}	ASDI ^{b)}	EXP ^{c)}
²⁴ Mg	2_1^+	1.37	-15 \pm 4	-16 \pm 1	-24 \pm 6 ^{d)}
²⁵ Mg	$5/2_1^+$	0	15 \pm 2	19 \pm 1	22 \pm 5
²⁶ Mg	2_1^+	1.81	\approx 0 \pm 18	-11 \pm 4	-14 \pm 5
²⁷ Al	$5/2_1^+$	0	13 \pm 2	16.3 \pm 0.5	15.1 \pm 0.3
²⁸ Si	2_1^+	1.78	15 \pm 2	16.4 \pm 0.5	16 \pm 3

a) $e^0 = 2.33 e$.b) $e^0 = 2.15 e$.

c) Ref. 9 unless indicated otherwise.

d) Ref. 10.

On inspection of tables 3.1 and 3.2 two conclusions can be drawn. In the first place there is a reasonable correlation between the size of the theoretical errors assigned and the deviation between theory and experiment. This was for the ASDI already mentioned in section 2 in connection with fig. 2.1. In the second place the ASDI results are generally better than the MSDI results. For 28 of the 62 transitions considered the ASDI showed a marked improvement over the MSDI results and for 6 matrix elements the opposite was the case.

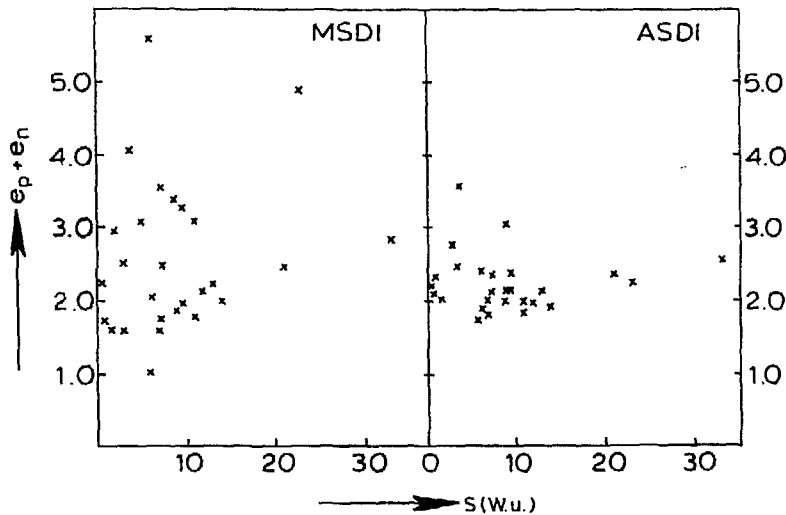


Fig. 3.4. The isoscalar effective charge reproducing the experimental strength for transitions between yrast levels.

An interesting difference between the E2 properties of ASDI and MSDI wave functions is shown in fig. 3.4. The abscissa of each cross represents the strength of a transition between yrast levels. The ordinate is the isoscalar effective charge e^0 needed to reproduce this strength theoretically. The spread is substantially smaller in the ASDI case. There is no reason to ascribe this smooth behaviour in the case of the ASDI to the fact that the yrast levels of all spins considered were used in the energy fit in [1].

In the remainder of this subsection we shall discuss some of the results presented in tables 3.1 and 3.2.

$A = 24$ The improvement of the ASDI over the MSDI is noteworthy, especially for the decay of the 4_1^+ level. Most of the ASDI wave functions do not differ very much from the corresponding MSDI wave functions; the 4_1^+ and 4_2^+ wave functions, however, become completely mixed.

A = 25 In ^{25}Mg and ^{25}Al one finds the strongest experimental E2 transitions of the A = 24 - 28 mass region. They are calculated too weak with both the MSDI and the ASDI wave functions. We have, however, some doubts about the accuracy of the experimental results for the case where agreement is worst, viz. the $5/2_2^+ \rightarrow 1/2_1^+$ transition in ^{25}Al . One needs a large isovector matrix element to explain the difference between the strengths of this transition and the analogous transition in ^{25}Mg . The required value of this isovector matrix element can easily be obtained by taking a linear combination of ASDI $1/2_1^+$ wave functions to represent the $1/2_1^+$ state and another linear combination of $5/2_2^+$ wave functions to represent the $5/2_2^+$ state. There is, however, no way of doing this without at the same time reducing the isoscalar contribution that must also be large to reproduce the data.

A = 26 The large difference between the ASDI and MSDI results for the quadrupole moment at the 2_1^+ level in ^{26}Mg are due to an accidental cancellation between large isoscalar and isovector contributions. Here it may be mentioned that the majority of the contributions to the right hand sides of the histograms in fig. 3.1 are from transitions in ^{26}Mg .

A = 27 Most of the results obtained for this mass are in very good agreement with experiment. We shall comment on the transition $5/2_2^+ \rightarrow 3/2_1^+$ in ^{27}Al and ^{27}Si in section 4.

A = 28 The $2_1^+ \rightarrow 0_1^+$ transition in ^{28}Si provides an example where, in the case of the ASDI, the equations (2.8) hold to a remarkable degree. Thus, since the $2_1^+ \rightarrow 0_1^+$ transition

exhausts virtually all E2 strength, and the energies are well reproduced, the resulting theoretical error assigned to this transition is very small.

3.3. M1 TRANSITIONS AND DIPOLE MOMENTS

3.3.1. *Effective M1 single-particle matrix elements.*

Although there is a tendency to calculate M1 strengths too large, the introduction of effective M1 single-particle matrix elements did not turn out to be very successful. This could be due to the fact that all first-order corrections to M1 single-particle matrix elements vanish because of l -forbiddenness.

A too strong dependence of the fitted SPME on the subset of the experimental data was found. If g -factors instead of single-particle matrix elements were fitted, this dependence turned out to be even stronger. Furthermore, the agreement obtained with fitted single-particle matrix elements was not much better than with bare-nucleon matrix elements. In the remainder of this paper we shall, in view of these observations, use bare-nucleon M1 single-particle matrix elements.

3.3.2. *Discussion of the M1 results.*

In this section we discuss some of the results displayed in tables 3.3 and 3.4. Comparing these tables with the analogous tables 3.1 and 3.2 for E2 transitions and quadrupole moments one sees that in general the relative theoretical errors assigned to M1 matrix elements are larger than those assigned to E2 matrix elements.

For 24 of the 56 matrix elements considered the ASDI showed a marked improvement over the MSDI results and in 15 cases the other way round. The agreement between experiment

and theory for M1 transitions is not as good as in the E2 case. Towards the higher part of the mass region the agreement obtained is in general better than for the lower masses. Very large differences are often visible between the ASDI and the MSDI results, this in spite of the large overlap between the low-lying ASDI and the corresponding MSDI wave functions.

Table 3.3

Comparison between experimental and calculated M1 transition strengths

		Transition		M1 Strength (cW.u.)					
		J_i^π, E_{x_i} (MeV)	J_f^π, E_{x_f} (MeV)	MSDI ^{a)}			ASDI ^{a)}		EXP ^{b)}
²⁴ Na	2_1^+	0.56	1_1^+	0.47	70	± 90	13	± 20	88 $\pm 11^c)$
²⁴ Mg	3_1^+	5.24	2_1^+	1.37	$(2\pm 4)\times 10^{-4}$		$(3\pm 20)\times 10^{-4}$		$(17\pm 8)\times 10^{-4}$
	1_1^+	7.75	0_1^+	0	0.05 ± 0.20		0.66 ± 0.09		0.15 ± 0.06
	1_2^+	9.83	0_1^+	0	0.4 ± 0.20		0.10 ± 0.07		5.5 ± 1.6
²⁵ Mg	$3/2_1^+$	0.97	$5/2_1^+$	0	0.5 ± 0.9		0.1 ± 0.3		$0.10 \pm 0.01^c)$
			$1/2_1^+$	0.59	2 ± 2		1.1 ± 1.0		$1.6 \pm 0.1^c)$
	$7/2_1^+$	1.61	$5/2_1^+$	0	11 ± 8		29 ± 4		$30 \pm 4^d)$
	$5/2_2^+$	1.96	$5/2_1^+$	0	$\approx 0 \pm 1$		0.02 ± 0.2		$0.08 \pm 0.03^d)$
			$3/2_1^+$	0.97	3 ± 5		3.1 ± 2.0		$1.0 \pm 0.4^d)$
	$1/2_2^+$	2.56	$1/2_1^+$	0.59	$\approx 0 \pm 20$		11 ± 6		5 ± 2
	$7/2_2^+$	2.74	$5/2_1^+$	0	8 ± 11		0.1 ± 0.4		$(3\pm 1)\times 10^{-3^d)}$

Table 3.3 (cont.)

Transition				M1 Strength (cW.u.)				
J_i^π , E_{xi} (MeV)	J_f^π , E_{xf} (MeV)			MSDI ^{a)}	ASDI ^{a)}	EXP ^{b)}		
^{25}Mg $7/2_2^+$	2.74	$5/2_2^+$	1.96	0.5 ± 2.0	0.3 ± 0.6	$1.2 \pm 0.3^{\text{d)}$		
$3/2_2^+$	2.80	$5/2_2^+$	1.96	4 ± 9	11 ± 4	7.2 ± 1.7		
$9/2_2^+$	4.06	$7/2_1^+$	1.61	7 ± 30	5 ± 8	1.5 ± 0.3		
^{25}Al $3/2_1^+$	0.94	$5/2_1^+$	0	0.9 ± 1.4	0.2 ± 0.5	0.23 ± 0.06		
		$1/2_1^+$	0.45	4 ± 3	2.5 ± 2.0	2.4 ± 0.6		
$5/2_2^+$	1.79	$5/2_1^+$	0	$\approx 0 \pm 6$	$\approx 0 \pm 0.7$	0.16 ± 0.04		
		$3/2_1^+$	0.94	4 ± 7	3.3 ± 2.0	3.5 ± 0.6		
^{26}Mg 2_2^+	2.94	2_1^+	1.81	35 ± 60	28 ± 20	25 ± 6		
3_1^+	3.94	2_1^+	1.81	6 ± 9	2 ± 3	0.19 ± 0.04		
		2_2^+	2.94	3 ± 7	14 ± 7	3.0 ± 0.7		
3_2^+	4.35	2_1^+	1.81	1 ± 4	0.8 ± 1.0	0.76 ± 0.10		
^{26}Al 1_1^+	1.06	$0_1^+, T=1$	0.23	100 ± 60	150 ± 20	140 ± 30		
1_2^+	1.85	$0_1^+, T=1$	0.23	6 ± 60	40 ± 20	19 ± 7		
$2_1^+, T=1$	2.07	1_1^+	1.06	60 ± 200	130 ± 30	$130 \pm 30^{\text{c)}$		
3_2^+	2.37	$2_1^+, T=1$	2.07	40 ± 100	60 ± 200	43 ± 9		
^{27}Mg $3/2_1^+$	0.98	$1/2_1^+$	0	2.7 ± 1.8	2.7 ± 1.0	2.3 ± 0.5		
^{27}Al $3/2_1^+$	1.01	$5/2_1^+$	0	2 ± 4	3.1 ± 1.0	1.4 ± 0.2		
		$1/2_1^+$	0.84	0.7 ± 1.0	11 ± 2	10 ± 1		

Table 3.3 (cont.)

		Transition		MI Strength (cW.u.)									
		J_i^-, E_{x_i} (MeV)	J_f^+, E_{x_f} (MeV)	MSDI ^{a)}		ASDI ^{a)}		EXP ^{b)}					
²⁷ Al	7/2 ₁ ⁺	2.21	5/2 ₁ ⁺	0	1.2	±	1.2	7.1	±	2.0	6.1	±	0.6
	5/2 ₂ ⁺	2.73	5/2 ₁ ⁺	0	~0	±	0.2	2	±	4	2.6	±	0.8
			3/2 ₁ ⁺	1.01	13	±	20	8	±	4	32	±	9
	3/2 ₂ ⁺	2.98	5/2 ₁ ⁺	0	27	±	10	33	±	5	20	±	2
	9/2 ₁ ⁺	3.00	7/2 ₁ ⁺	2.21	21	±	4	19	±	5	7.0	±	1.7
	11/2 ₁ ⁺	4.51	9/2 ₁ ⁺	3.00	5	±	4	0.5	±	2.0	0.57	±	0.07 ^{f)}
	7/2 ₂ ⁺	4.58	5/2 ₁ ⁺	0	6	±	9	4	±	3	1.3	±	0.4
			7/2 ₁ ⁺	2.21	1	±	7	5	±	4	1.9	±	0.7
	9/2 ₂ ⁺	5.43	7/2 ₁ ⁺	2.21	~0	±	0.5	8	±	4	1.0	±	0.3
	²⁷ Si	3/2 ₁ ⁺	0.96	5/2 ₁ ⁺	0	2	±	3	4.1	±	1.0	1.8	±
7/2 ₁ ⁺		2.16	5/2 ₁ ⁺	0	0.8	±	0.9	5	±	2	5.2	±	0.7
5/2 ₂ ⁺		2.65	5/2 ₁ ⁺	0	~0	±	0.4	0.7	±	0.8	1.1	±	0.5
			3/2 ₁ ⁺	0.96	11	±	18	6	±	3	21	±	8
²⁸ Al	2 ₁ ⁺	0.03	3 ₁ ⁺	0	80	±	20	34	±	6	37	±	1
	3 ₂ ⁺	1.01	3 ₁ ⁺	0	8	±	30	6	±	4	8.6	±	1.3
			2 ₁ ⁺	0.03	8	±	15	18	±	6	16	±	2
	1 ₁ ⁺	1.37	2 ₁ ⁺	0.03	1	±	5	5	±	6	2.2	±	0.4
			0 ₁ ⁺	0.97	80	±	100	60	±	30	68	±	14

Table 3.3 (cont.)

	Transition				M1 Strength (cW.u.)		
	J_i^π, E_{x_i} (MeV)	J_f^π, E_{x_f} (MeV)	MSDI ^{a)}	ASDI ^{a)}	EXP ^{c)}		
²⁸ Al	1_2^+ 1.62	2_1^+ 0.03	1 ± 7	12 ± 8	3.9 ± 0.9		
²⁸ Si	3_1^+ 6.27	2_1^+ 1.78	$(13 \pm 5) \times 10^{-2}$	$(5 \pm 5) \times 10^{-3}$	$(26 \pm 3) \times 10^{-3}$		

a) Bare-nucleon M1 single-particle matrix elements.

b) Experimental data from [7,8]; more recent data taken into account are quoted explicitly.

c) Ref. 12. d) Ref. 22. e) Ref. 23. f) Ref. 24.

Table 3.4

Comparison between experimental and calculated magnetic dipole moments

	J_i^π, E_{x_i} (MeV)	μ (n.m)		
		MSDI ^{a)}	ASDI ^{a)}	EXP ^{b)}
²⁴ Mg	2_1^+ 1.37	1.07 ± 0.01	1.07 ± 0.01	$1.02 \pm 0.04^c)$
²⁵ Mg	$5/2_1^+$ 0	-0.61 ± 0.09	-0.94 ± 0.10	$-0.86^e)$
²⁶ Mg	2_1^+ 1.81	1.1 ± 1.7	1.9 ± 0.4	$1.6 \pm 0.3^d)$
²⁷ Al	$5/2_1^+$ 0	3.9 ± 0.1	4.2 ± 0.1	$3.64^e)$
²⁸ Al	3_1^+ 0	3.2 ± 0.3	4.0 ± 0.1	$2.79^e)$
	2_1^+ 0.03	4.0 ± 0.2	3.7 ± 0.2	4.3 ± 0.4
²⁸ Si	2_1^+ 1.78	1.06 ± 0.01	1.08 ± 0.01	$1.12 \pm 0.18^d)$

a) Bare-nucleon M1 single-particle matrix elements.

b) Experimental data from ref. 9 unless indicated otherwise.

c) Ref. 13. d) Ref. 14. e) Experimental error is negligible.

We shall now discuss some of the cases presented in tables 3.3 and 3.4.

The ASDI wave functions to describe ^{24}Na and ^{24}Al are of very poor quality when compared with the MSDI wave functions. This might be due to the fact that in the construction of the ASDI matrix elements the equations for ^{24}Na had a small weighting factor.

The experimental strength of the $1_2^+ \rightarrow 0_1^+$ transition in ^{24}Mg cannot be reproduced in the given configuration space. This was checked by the use of the method described in [5]. Since the energy difference between this 1_2^+ state and the 1_1^+ , $T = 1$ state amounts to only 0.14 MeV, an easy explanation of the discrepancy is to be found in isospin mixing [8].

In CTME between levels in ^{26}Mg or ^{26}Si one encounters the largest M1 isoscalar contributions for the mass region under consideration. This applies especially to matrix elements between states with the same spin. An analogous anomaly, regarding exceptionally large E2 isovector matrix elements, was mentioned before. In section 4 we shall discuss an interesting combination of these effects, viz. the mixing ratios in ^{26}Mg and ^{26}Si . Most of the M1 transitions in $A = 27$ are reproduced reasonably well, the worst exception being the $5/2_2^+ \rightarrow 3/2_1^+$ transitions in both ^{27}Al and ^{27}Si . We shall comment on these transitions in section 4.

The M1 decay rates in $A = 28$ are calculated as well as can be expected from the calculated errors. The erroneous result for the magnetic moment of the 3_1^+ state in ^{28}Al is at present not well understood. A large mixing with the 3_2^+ state is required to obtain the experimental result, but this would at the same time spoil the agreement obtained for the other properties involving the 3_1^+ state.

4. Gamma-decay schemes

In the remainder of this paper we shall concentrate on the results obtained with the ASDI wave functions since, as was shown in section 3, they are superior to the MSDI wave functions. In line with the discussion presented in section 3 we shall use a state independent effective charge of $e^0 = 2.15e$ for the isoscalar matrix elements of the E2 operator and bare-nucleon matrix elements for the M1 operator.

The quantities we shall consider are mixing and branching ratios and lifetimes. These depend not only on transition matrix elements but also on energy differences. For these energy differences we use throughout the experimental values. There are two reasons for considering all these quantities instead of only transition matrix elements as in section 3. The first reason is that comparatively few of the latter can be extracted meaningfully from the large amount of available data presented in [9]. Too large experimental errors would result, thus rendering a comparison with theory useless. The second reason will be dealt with in the next subsection.

4.1. ASSIGNMENT OF ERRORS TO QUANTITIES DEPENDING ON SEVERAL MATRIX ELEMENTS

For a proper assignment of errors to quantities that depend on more than one transition matrix element the procedure followed up to now needs some extension. Let a quantity $G(e_\alpha, m_\alpha)$ be a function of E2 and M1 matrix elements e_α and m_α , respectively, with $\alpha = 1, 2, \dots$. A small change δH in the Hamiltonian will cause the change

$$\delta G = \sum_{\alpha} \left(\frac{\partial G}{\partial e_{\alpha}} \delta e_{\alpha} + \frac{\partial G}{\partial m_{\alpha}} \delta m_{\alpha} \right). \quad (4.1)$$

The changes δe_{α} and δm_{α} , given by eq. (2.2) in terms of the matrix elements of δH , are in general not independent. After insertion of eq. (2.2) into eq. (4.1) and after taking together the coefficients that multiply the same matrix element of δH , one may proceed in exactly the same way as in section 2 to obtain the error in G.

If one follows this procedure it turns out that in many cases the resulting error is smaller than the one obtained by ignoring the coherence contributing terms. This remark applies in practice especially to the E2/M1 mixing ratios. Under a change δH the ratio $(e + \delta e)/(m + \delta m)$ will be fairly constant in many cases.

We calculated, in the way described above, the errors in the following quantities: mixing and branching ratios, lifetimes and ratios of partial widths. These have one thing in common in that they all involve matrix elements referring to one and the same initial state. One quantity that could be of interest is left for future consideration. It concerns the ratio $\Gamma(a \rightarrow b) / \Gamma(b \rightarrow c)$, i.e. the ratio between two strengths following each other in a cascade. Such transitions also have one state, b, in common.

4.2. RESULTS

In this sub-section we discuss the results displayed in figs. 4.1 to 4.11. In these figures the positive-parity states for the nuclei considered are included, with the following restrictions. i) Only up to three eigenvectors of a certain spin value are used since the higher eigenvectors

are very unreliable, as was discussed before. ii) Only those states are given whose spin and eigenvector were unambiguously known.

Calculated branching ratios are given when they amount to 1 % or more. Calculated mixing ratios are given if the experimental mixing ratio is known or if the experimental branching ratio is larger than 10 %. We did not venture to calculate M3/E2 mixing ratios for the mass region under consideration since none of them is experimentally known to be different from zero with any degree of precision. Moreover, a reasonable estimate for a renormalized M3 operator is not available. Theoretical errors are quoted in figs. 4.1 to 4.11 if two conditions are satisfied: i) the calculated error is smaller than the value itself; ii) the eigenvector numbers of the states J_m^π involved obey $m \leq 2$.

4.2.1. *Lifetimes*. An impression of the overall agreement between experiment and the results of the calculations with ASDI wave functions can be obtained from table 4.1. In this table we give for each mass the weighted average of the ratio between the experimental and the calculated lifetimes. The weighting factor of each ratio was calculated by adding quadratically the experimental and theoretical errors. Table 4.1 shows that for the lifetimes considered the agreement is in general very good. There is a slight tendency to overestimate the lifetimes, but even for the worst case, $A = 26$, the deviations are hardly meaningful. The averaging was done over all those lifetimes for which the experimental and the theoretical error were both smaller than the values themselves. Most of the lifetimes excluded from the averaging procedure showed too large a theoretical error. Thus a large

number of lifetimes are excluded, as can be seen in the third column of table 4.1. We conclude that lifetimes are often sensitive to the precise choice of the Hamiltonian.

Table 4.1

The average ratio between experimental and calculated lifetimes

MASS	$\tau_{\text{exp}}/\tau_{\text{th}}$	N_c/N
24 ^{a)}	1.05 ± 0.11	4/8
25	0.91 ± 0.15	4/15
26	0.82 ± 0.08	10/21
27	0.93 ± 0.07	14/16
28 ^{b)}	0.98 ± 0.09	4/15
total ^{a,b)}	0.92 ± 0.04	36/75

N_c : the number of lifetimes for which the relative experimental and theoretical errors are less than 100%. The average is taken over these cases only.

N : the number of lifetimes for which the relative experimental error is less than 100%.

a) $2_1^+ \rightarrow 0_1^+$ transition in ^{24}Mg omitted (weight too large).

b) $2_1^+ \rightarrow 0_1^+$ transition in ^{28}Si omitted (weight too large).

We shall now discuss some particular cases. Some striking discrepancies will be discussed in connection with mixing ratios.

The lifetime of the 0_2^+ level at 3.59 MeV in ^{26}Mg . The lifetime calculated far too large for this state results from an accidental cancellation between isoscalar and isovector E2 matrix elements. This can be seen clearly if one makes a comparison with the lifetime of the corresponding level in ^{26}Si . Small admixture of the 0_1^+ state in the 0_2^+ state would decrease considerably the lifetimes for both the 0_2^+ states in ^{26}Mg and ^{26}Si . Possible inaccuracies of the $2_{1,2}^+$ wave functions will be discussed in the next sub-section.

The lifetime of the 1_2^+ and 1_3^+ levels in ^{26}Al at 1.85 and 2.07 MeV, respectively. It was found on inspection that small changes in the Hamiltonian tend to worsen the poor agreement with experiment still further.

4.2.2. *E2/M1 mixing ratios.* In table 4.2 we show the weighted average of $\delta(\text{exp})/\delta(\text{th})$, the ratio between the experimental and calculated mixing ratios. The procedure followed was the same as for table 4.1. Some values of $\delta(\text{exp})/\delta(\text{th})$ were not included in the averaging procedure since they differed greatly from the average value of the remaining cases; they will be discussed in detail below.

As one sees from table 4.2, the agreement is in general very good. It was mentioned before that one often finds surprisingly small theoretical errors for E2/M1 mixing ratios. It should also be noted that, when compared with lifetimes, relatively few cases had to be excluded from the averaging procedure because the theoretical errors are too large. This indicates that the results had a relatively weak dependence

Table 4.2

The average ratio between experimental and calculated mixing ratios

MASS	$\delta_{\text{exp}}/\delta_{\text{th}}$	N_c/N
24		0/2
25	1.09 ± 0.09	9/15
26 ^{a)}	1.1 ± 0.3	1/3
27 ^{b)}	1.04 ± 0.08	8/9
28	0.9 ± 0.4	3/3
total ^{a,b)}	1.06 ± 0.06	21/34

See caption for Table 4.1 with "mixing ratio" replacing "lifetime".

a) $\delta(2_2^+ \rightarrow 2_1^+)$ in ^{26}Si omitted.

b) $\delta(5/2_2^+ \rightarrow 3/2_1^+)$ in ^{27}Al and ^{27}Si omitted (weight too large).

on the choice of the Hamiltonian. Indeed it was found that the results, when compared with earlier calculations (see e.g. [15]), did not show any dramatic improvement.

We shall now discuss some particular cases shown in figures 4.1 to 4.11. The phase convention for the mixing ratio is that of Brink and Rose [16].

In only two cases was the experimental sign reproduced improperly. In one of them, viz. $\delta(2_2^+ \rightarrow 2_1^+)$ in ^{24}Mg , extremely small changes in the wave functions would give agreement with experiment. The second case where the sign of the mixing ratio was not reproduced, i.e. $\delta(2_2^+ \rightarrow 2_1^+)$ in ^{26}Si , deserves closer attention. This is one of the two cases where we

assigned a small error to a completely wrong result. The mixing ratio for the analogous transition in ^{26}Mg is well reproduced. The calculated result follows the normal pattern, i.e. the E2/M1 mixing ratios of analogous transitions have opposite signs. In view of the small theoretical error we conclude that

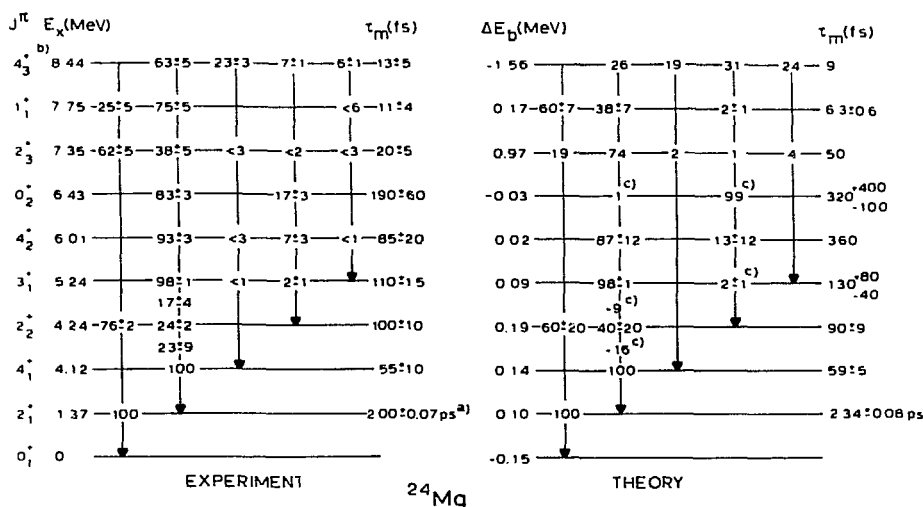


Fig. 4.1 Comparison between the experimental and the calculated decay scheme for positive parity states with low spin values. Lifetimes, branchings and E2/M1 mixing ratios are given; ΔE_b represents the difference between the experimental and calculated energies. Experimental data are from [9] unless indicated otherwise. Calculated results were obtained with the ASDI wave functions, bare-nucleon M1 single-particle matrix elements and an isoscalar effective charge $e^0 = 2.15 e$. The convention for quoting theoretical errors is given in the text.

a) Ref. 11. b) 1% branch to 3_1^- state. c) Discussed in the text.

the configuration space used was not appropriate to describe both the 2_1^+ and the 2_2^+ states. Especially in this case this conclusion could be made plausible even without using the ansatz 2.5 that underlies our error calculations. It turned out that all unitary transformations among the first four 2^+ states yielded an even more negative value of the mixing ratio $\delta(2_2^+ \rightarrow 2_1^+)$ in ^{26}Si if at the same time the large strengths of the $2_1^+ \rightarrow 0_1^+$ transitions in ^{26}Mg and ^{26}Si were maintained. Mixing with states 2_m^+ ($m \geq 5$) would decrease still further the strengths of the $2_1^+ \rightarrow 0_1^+$ and $2_2^+ \rightarrow 0_1^+$ transitions in ^{26}Mg that were calculated too weak already. Equivalently, cf. eq. (2.7), it was found that off-diagonal matrix elements of δH to the high-lying states of the order 1.0 MeV were needed to influence the strengths of the $2_1^+ \rightarrow 0_1^+$ transition to any substantial extent.

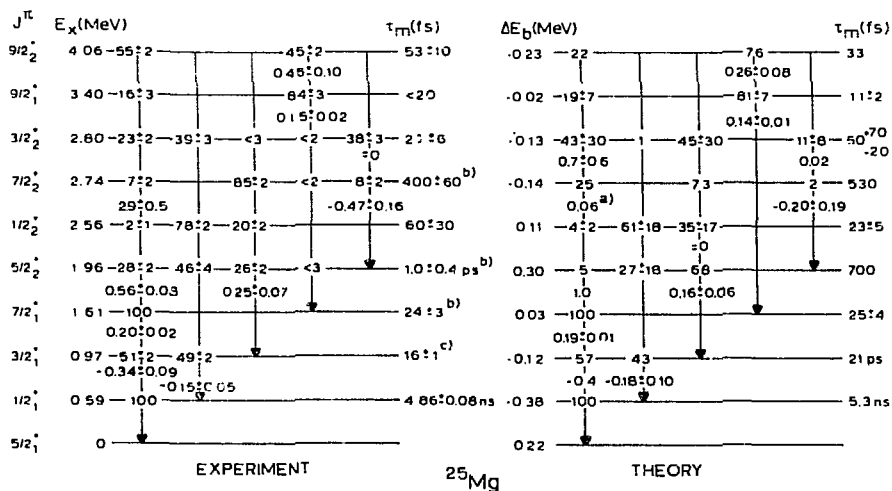


Fig. 4.2. See caption for fig. 4.1.

a) Discussed in the text. b) Ref. 22. c) Ref. 12.

There is one more case, viz. $\delta(5/2_2^+ \rightarrow 3/2_1^+)$ in ^{27}Al and ^{27}Si , where a serious discrepancy between theory and experiment occurs. This discrepancy is due to too small a value for the calculated MI matrix element. The rather small errors that are assigned to this mixing ratio and to the lifetime of the $5/2_2^+$ level indicate that one cannot expect too much from changes in the Hamiltonian. It is not clear at present if the appropriateness of the configuration space should be questioned or if a reasonable Hamiltonian reproducing the data can still be found.

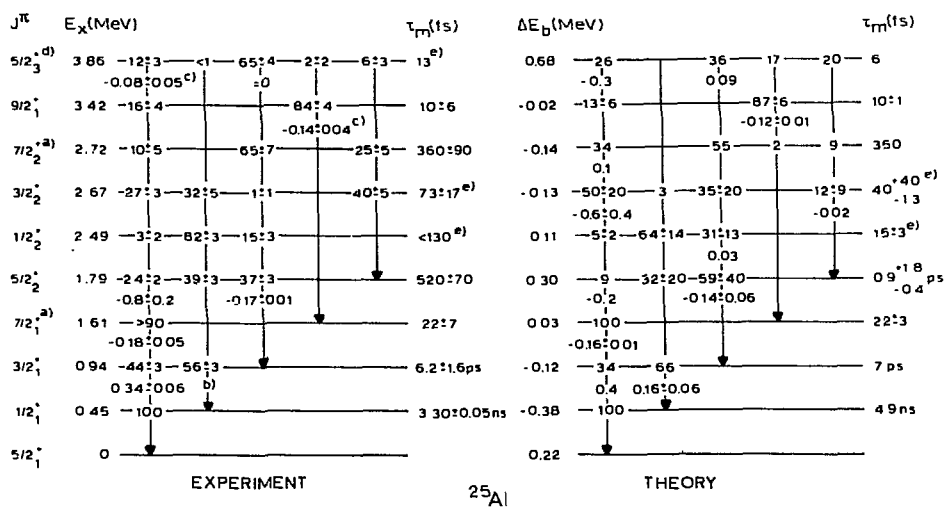


Fig. 4.3. See caption for fig. 4.1.

- Spin not known within 0.1 % confidence limit.
- $\delta = 0.05 \pm 0.04$ or $\delta = -0.15 \pm 0.05$ are quoted in [9].
- Erroneous sign quoted in [9].
- Branches to high lying states not displayed.
- Partial lifetimes h/Γ_γ .

In the other cases where theory and experiment are in disagreement, the theoretical results turned out to be very sensitive to little admixtures of other states. For example, $\delta(7/2_2^+ \rightarrow 5/2_1^+)$ in ^{25}Mg will be in agreement with experiment if one mixes 0.2 % of the $7/2_1^+$ wave function into the $7/2_2^+$ wave function.

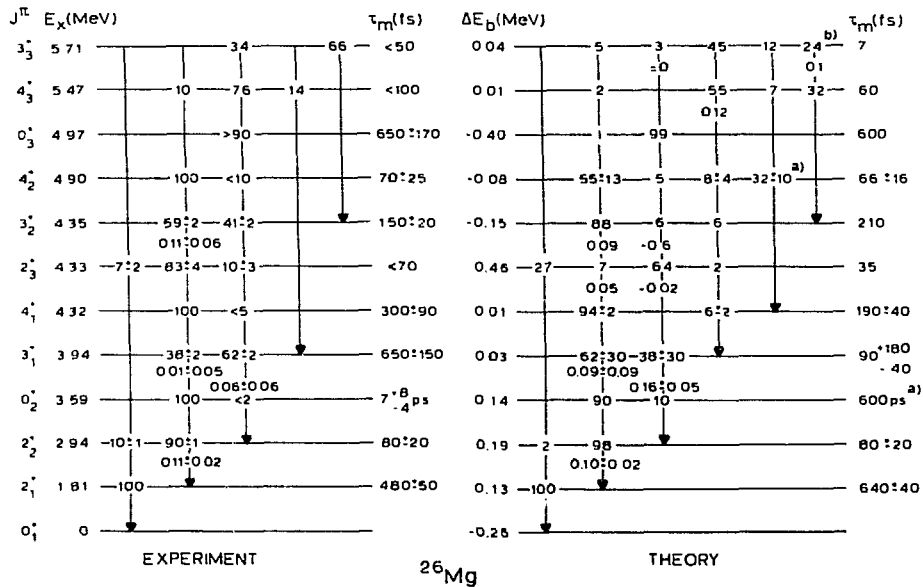


Fig. 4.4. See caption for fig. 4.1.

a) Discussed in the text.

b) 11 % branch to 2_3^+ state not shown.

4.2.3. *Branching ratios.* The overall agreement obtained for branching ratios is quite satisfactory although it is not as good as for lifetimes and mixing ratios. In most cases there is still a reasonable correlation between the agreement obtained and the theoretical errors assigned. The errors found, however, are often large, indicating the sensitivity of the result for the choice of the Hamiltonian. This may seem remarkable since one would expect branching ratios to be determined largely by the high powers of energy differences that enter the relevant formulae. If however one notes that mixing

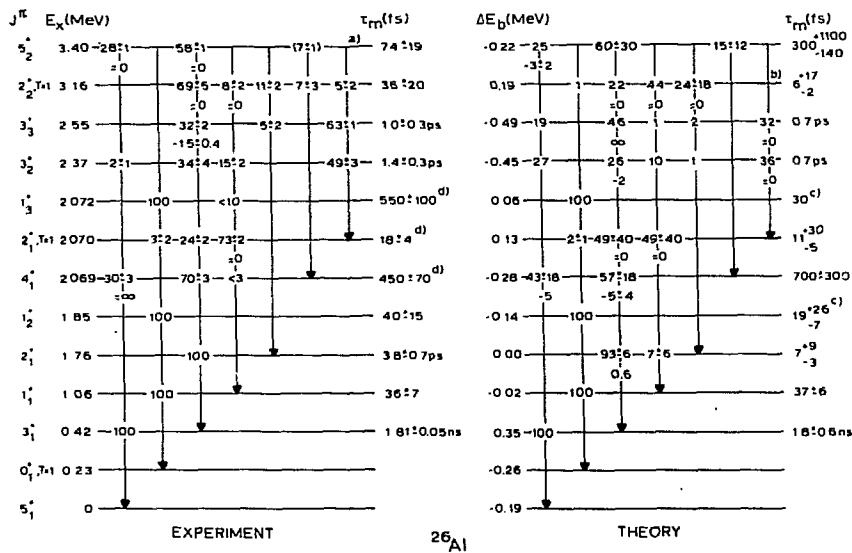


Fig. 4.5. See caption of fig. 4.1.

- a) 7±2 % branch to 3_3^+ level not shown.
- b) 5 % branch to 1.85 MeV level not shown; another 4 % is fragmented over many higher states.
- c) Discussed in the text.
- d) Ref. 23.

ratios are quite insensitive to changes in the Hamiltonian, as was shown before, it will be clear that at the same time partial widths of mixed transitions will be particularly sensitive to changes in the Hamiltonian.

We shall now discuss some special cases.

The 3_1^+ state in ^{24}Mg at 5.24 MeV. The properties of this state are well reproduced. It is interesting to note that the calculated E2 strength for the transition to the 2_2^+ state at 4.24 MeV is the largest found in the mass region under consideration, viz. 24 ± 3 W.u. Experimental information about the mixing ratio of this weak branch is lacking however. The calculation yields a nearly pure E2 character for this transition.

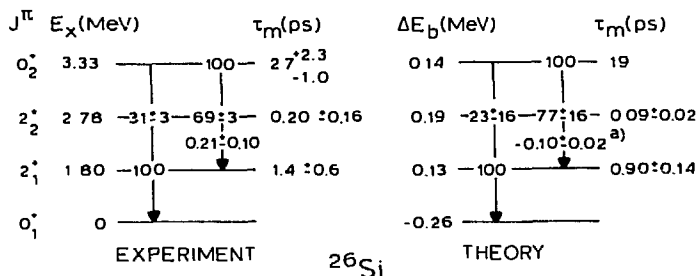


Fig. 4.6. See caption of fig. 4.1.

a) M3/E2 mixing ratio: 0.14 ± 0.19 .

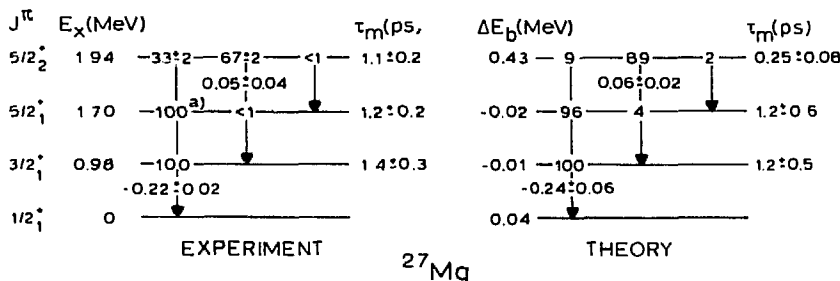


Fig. 4.7. See caption fig. 4.1.

a) M3/E2 mixing ratio: 0.14 ± 0.19 .

The 0_2^+ state at 6.43 MeV in ^{24}Mg . The ratio $\Gamma(0_2^+ \rightarrow 2_1^+)/\Gamma(0_2^+ \rightarrow 2_2^+)$ depends strongly on the choice of the Hamiltonian. In fact an admixture of 5 % of the 2_1^+ state and the 2_2^+ state into each other would give agreement with experiment. As a by-product of this transformation it is then found that the lifetime of the 2_1^+ state comes out in agreement with the experimental value.

The 4_2^+ state at 4.90 MeV in ^{26}Mg . An improbably large mixing of the 4^+ states is needed to suppress the large calculated MI matrix element of the transition to the 4_1^+ level at 4.32 MeV. No experimental upper limit is, however, available for this unobserved branch.

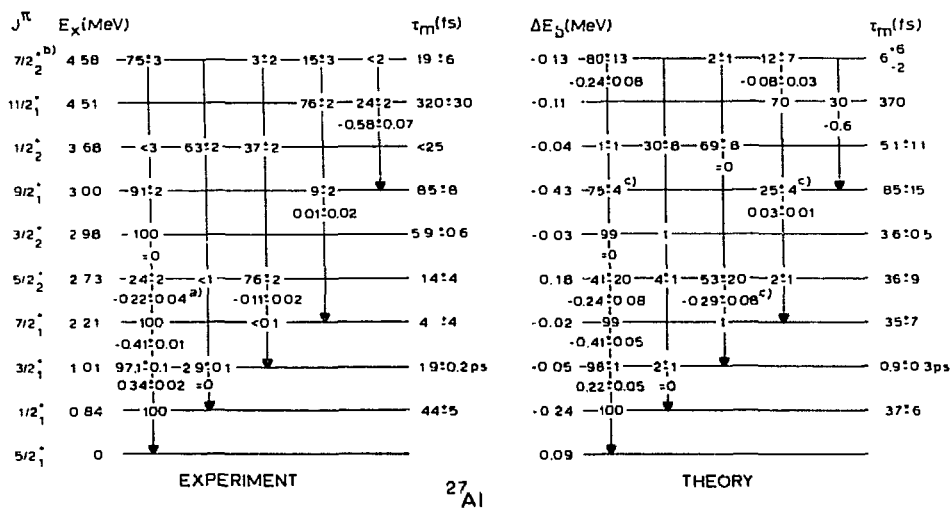


Fig. 4.8. See caption of fig. 4.1.

a) Ref. 25.

b) Branch to 2.73 MeV level; exp.: 7 ± 2 %, calc.: 6 ± 6 %.

c) Discussed in the text.

d) Ref. 24.

The $9/2_1^+$ state at 3.00 MeV in ^{27}Al . The decay of this state provides one of the few cases where the branching ratios are more stable under changes of the Hamiltonian than the matrix elements involved.

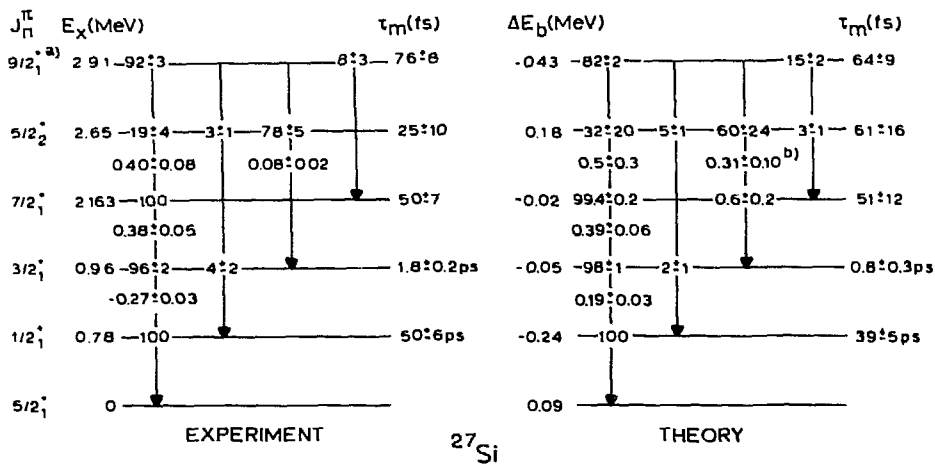


Fig. 4.9. See caption of fig. 4.1.
 a) Spin assignment from [20].
 b) Discussed in the text.

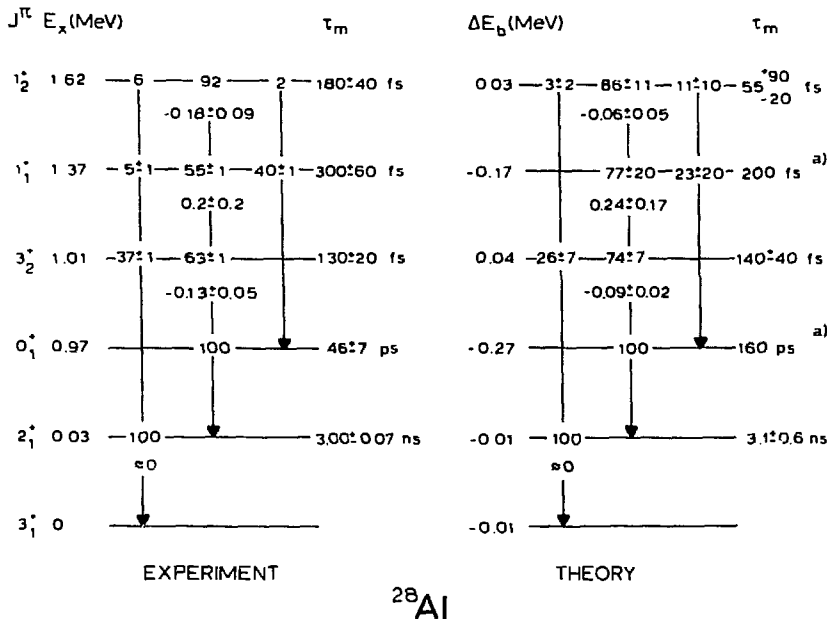


Fig. 4.10. See caption of fig. 4.1.

The 2_2^+ and 2_3^+ states at 7.38 and 7.42 MeV. In section 2 we noted already that the assignment of these two experimental states to the calculated ones was erroneous. Let us consider linear combinations of the calculated 2_2^+ and the 2_3^+ states of the form:

$$\begin{aligned} |2_2^{+'}> &= 0.6|2_2^+> + 0.8|2_3^+>, \\ |2_3^{+'}> &= -0.8|2_2^+> + 0.6|2_3^+>. \end{aligned} \quad (4.2)$$

This means that the two states are to a large extent interchanged. The properties of the new states $|2_2^{+'}>$ and $|2_3^{+'}>$ are in amazing agreement with experiment, as shown in table 4.3. The experimental values of the E2 matrix elements for the transitions $2_{2,3}^+ \rightarrow 2_1^+$ were obtained on the assumption that the purely isoscalar M1 matrix elements could be neglected.

Clearly we now have a set of good wave functions, without however knowing a Hamiltonian of which they are the eigenfunctions

Table 4.3

Decay of the 2_2^+ and the 2_3^+ states in ^{28}Si

i	→	f	$\langle f 0(E2) i \rangle$ (efm ²)		
			Exp.	ASDI	Mixed ^{a)}
2_2^+	→	0_1^+	3.0 ± 0.4	-3.5	-3.1
		2_1^+	$7.3 \pm 1.1^{\text{b)}$	4.0	6.1
		0_2^+	c)	6.8	0.5
2_3^+	→	0_1^+	2.2 ± 0.1	-1.3	2.1
		2_1^+	$0.8 \pm 0.3^{\text{b)}$	4.6	-0.5
		0_2^+	9.6 ± 1.9	-4.5	-8.1

a) C.f. eq. (4.2).

b) Pure E2 character assumed.

c) Not observed.

The 1_1^+ level at 8.33 MeV in ^{28}Si . The calculated branching ratios are very sensitive to admixtures of higher 1^+ states; small admixtures of the 1_2^+ state give agreement with experiment. To reproduce the experimental lifetime, however, a nearly complete interchange of the 1_1^+ and 1_3^+ wave functions is required. It is concluded that either the experimental lifetime is about one order of magnitude too large, or we have here an interesting case for future theoretical consideration.

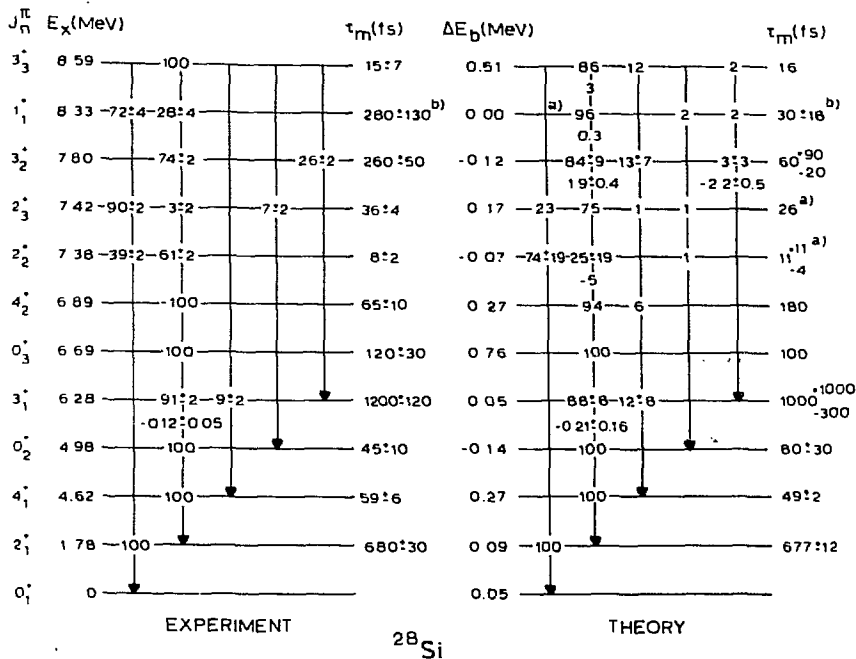


Fig. 4.11. See caption of fig. 4.1.

- a) Discussed in the text.
- b) Ref. 21.

5. Predictions for static moments.

In this section we present predictions for magnetic dipole moments and electric quadrupole moments. The calculations were performed with ASDI wave functions.

5.1. MAGNETIC DIPOLE MOMENTS

Magnetic dipole moments were calculated with the bare-nucleon M1 single-particle matrix elements. In table 5.1 the predictions for the magnetic moments and their theoretical errors are shown for a number of states. The table includes only those states whose moment one would expect to be measurable by present-day techniques. This implies that i) only states with a lifetime $\tau_m \gtrsim 0.3$ ps are considered and ii) only the first few, i.e. about five levels of each nucleus are considered. It should be mentioned that particularly in the case of magnetic moments the assigned theoretical errors tend to be quite small. This is because eq. (2.8) is satisfied to a remarkable degree. As yet there is no satisfactory explanation for this phenomenon.

5.2. ELECTRIC QUADRUPOLE MOMENTS

Electric quadrupole moments were calculated with an isoscalar effective charge $e^0 = 2.15 e$. Table 5.2 shows the results. For the β -instable nuclei we give the quadrupole moment of the ground state only. Theoretical errors were not quoted if they turned out to be larger than 100 %. The large errors were in all cases due to very big E2 matrix elements of the type $\langle J_1^\pi | 0(E2) | J_2^\pi \rangle$.

Table 5.1

The ASDI predictions for magnetic dipole moments

J^π, E_x (MeV)			μ (n.m)	J^π, E_x (MeV)			μ (n.m)
^{25}Mg	$1/2_1^+$	0.59	- 0.2	^{27}Mg	$1/2_1^+$	0	-0.36 ± 0.03
	$3/2_1^+$	0.97	0.99 ± 0.18		$3/2_1^+$	0.98	1.74 ± 0.16
	$5/2_2^+$	1.96	0.40 ± 0.12		$5/2_1^+$	1.70	0.1
^{25}Al	$5/2_1^+$	0	3.83 ± 0.12	^{27}Al	$5/2_2^+$	1.94	1.13 ± 0.63
	$1/2_1^+$	0.45	0.8 ± 0.2		$1/2_1^+$	0.84	2.61 ± 0.04
	$3/2_1^+$	0.95	0.52 ± 0.18		$3/2_1^+$	1.01	1.48 ± 0.06
^{26}Mg	$5/2_2^+$	1.79	2.49 ± 0.13	^{27}Si	$5/2_1^+$	0	-1.28 ± 0.06
	3_1^+	3.94	1.7 ± 0.7		$1/2_1^+$	0.78	-1.80 ± 0.04
	^{26}Al	5_1^+	0		2.9 ± 0.01	$3/2_1^+$	0.96
3_1^+		0.42	1.82 ± 0.04	^{28}Al	1_1^+	1.37	0.87 ± 0.10
2_1^+		1.76	1.18 ± 0.03		^{28}Si	3_1^+	6.28
^{26}Si	2_1^+	1.80	0.3	^{28}P		3_1^+	0

Table 5.2

The ASDI predictions for electric quadrupole moments

	$J^\pi, E_x(\text{MeV})$	$Q(\text{efm}^2)$		$J^\pi, E_x(\text{MeV})$	$Q(\text{efm}^2)$
^{25}Mg	$3/2_1^+$ 0.97	-11.6 ± 0.2	^{28}Al	3_1^+ 0	16.1 ± 0.3
	$5/2_2^+$ 1.96	-14 ± 2	^{28}Si	4_1^+ 4.62	18.6 ± 1.2
^{25}Al	$5/2_1^+$ 0	17.1 ± 1.3		3_1^+ 6.28	9 ± 3
^{26}Mg	3_1^+ 3.94	$1^{\text{a)}}$		4_2^+ 6.89	4 ± 3
	4_1^+ 4.32	$2^{\text{a)}}$		2_2^+ 7.38	8 ± 8
^{26}Al	5_1^+ 0	25.7 ± 0.7			$-11^{\text{b)}}$
^{27}Al	$3/2_1^+$ 1.01	-12.6 ± 0.1		2_3^+ 7.42	-9 ± 7
	$7/2_1^+$ 2.21	8.4 ± 0.4			$9^{\text{b)}}$
	$9/2_1^+$ 3.00	23.8 ± 0.4	^{28}Al	3_1^+ 0	16.1 ± 1.3
^{27}Si	$5/2_1^+$ 0	13.0 ± 0.7	^{28}P	3_1^+ 0	13.1 ± 1.5

a) Extremely sensitive to admixtures of other states with the same spin.

b) Values obtained with mixed states defined in eq. (4.2).

6. Allowed β -decay

In this section we present $\log ft$ values for allowed β -decay calculated with ASDI wave functions.

The ft value of a transition from an initial state $|I\rangle$ to a final state $|F\rangle$ is defined as:

$$ft = \frac{2\pi^3 \hbar^7 \ln 2}{m^5 c^4} \{G_V^2 \langle 1 \rangle^2 + G_A^2 \langle \sigma \rangle^2\}^{-1} \quad (6.1)$$

where $\langle 1 \rangle$ and $\langle \sigma \rangle$ denote the usual Fermi and Gamov-Teller matrix elements.

For the vector coupling constant, G_V , we shall adopt the value:

$$G_V^2 = 2.00 \times 10^{-98} \text{ erg}^2 \text{ cm}^6. \quad (6.2)$$

With this choice of G_V^2 one obtains a good fit to the ft values for the pure Fermi transitions $0^+ \rightarrow 0^+$ of ^{14}O and $^{26}\text{Al}^m$.

A proper choice of G_A is less trivial. The ratio G_A^2/G_V^2 for free neutron decay is experimentally known to be 1.53. A value of 1.29 for this ratio is obtained by Wilkinson [17] from a fit to odd-mass nuclei with $A = 11 - 21$. We shall use the latter value for the presentation of our results. On insertion of the numerical values of all constants the expression (6.1) therefore becomes:

$$ft = \frac{6155}{\langle 1 \rangle^2 + 1.29 \langle \sigma \rangle^2} \text{ s.} \quad (6.3)$$

We also considered the ratio G_A/G_V as a free parameter in order to obtain the value that would best fit our results

to the experimental data; the fitting procedure used is described in section 3. In this way it was found that the surprisingly low value $G_A^2/G_V^2 = 0.65$ gives best agreement. It is seen that for the mass region under consideration a large reduction of the axial vector coupling constant is required.

It should be mentioned, however, that part of the large reduction factor might be due to deficiencies in our wave functions. The calculation of spectroscopic factors in [1] indicated that the $d_{3/2}$ content is too small. The Gamow-Teller matrix elements are more sensitive to the $d_{3/2}$ content than the observables discussed up to now. On decreasing the $d_{5/2}$ - $d_{3/2}$ spin-orbit splitting one enlarges the $d_{3/2}$ content of the wave functions and decreases the Gamow-Teller matrix element. The precise argument leading to this last conclusion is discussed in detail in [18] and will not be repeated here. The same point was also stressed in another recent calculation of allowed β -decay in the s-d shell [19].

The results of our calculations are presented in table 6.1. The experimental $\log ft$ values are taken from [9]. The effect of using the fitted value $G_A^2/G_V^2 = 0.65$ would be to enlarge the $\log ft$ values of the pure Gamow-Teller transitions by the amount 0.30; the $\log ft$ value of the two mixed transitions, i.e. the $^{25}\text{Al} \rightarrow ^{25}\text{Mg}$ and the $^{27}\text{Si} \rightarrow ^{27}\text{Al}$ ground state transition increase by 0.12 and 0.14, respectively.

The convention for quoting theoretical errors is as before. As seen from table 6.1, in many cases the theoretical errors are not sufficiently large to explain the often large (and positive) differences between the experimental and calculated $\log ft$ values. Thus we conclude that it will be difficult to find a Hamiltonian in the given configuration space that will

yield good agreement with experiment. This seems to contradict our previous remark that when the spin-orbit splitting is diminished, the calculated Gamow-Teller matrix elements will decrease. One should however bear in mind that in doing this a drastic change of our configuration space will result as a consequence of the procedure followed in [1] for determining the configuration space.

Table 6.1

Comparison between calculated and experimental log ft values for allowed β -decay

				log ft		
	J_i^π		J_f^π	E_{xf} (MeV)	ASDI ^{a)}	EXP ^{b)}
^{24}Na	4_1^+	^{24}Mg	4_1^+	4.12	5.6	6.12 ± 0.02
			3_1^+	5.24	$6.0 \begin{smallmatrix} + 0.5 \\ - 0.2 \end{smallmatrix}$	6.77 ± 0.04
^{24}Al	4_1^+	^{24}Mg	4_1^+	4.12	5.6	6.2 ± 0.2
			3_1^+	5.24	$6.0 \begin{smallmatrix} + 0.5 \\ - 0.2 \end{smallmatrix}$	6.49 ± 0.17
			4_2^+	6.01	3.6 ± 0.2	6.4 ± 0.2
			4_3^+	8.44	4.8	3.99 ± 0.05
^{24}Al	1_1^+	^{24}Mg	0_1^+	0	4.2 ± 0.2	6.01 ± 0.15
			2_1^+	1.37	4.34 ± 0.15	6.18 ± 0.15
			2_1^+	4.24	$5.2 \begin{smallmatrix} + 1.0 \\ - 0.4 \end{smallmatrix}$	6.07 ± 0.15
^{25}Na	$5/2_1^+$	^{25}Mg	$5/2_1^+$	0	4.6 ± 0.2	5.25 ± 0.02
			$3/2_1^+$	0.97	4.9 ± 0.2	5.05 ± 0.03
			$7/2_1^+$	1.61	4.7 ± 0.2	5.03 ± 0.03
			$5/2_2^+$	1.96	5.8	5.99 ± 0.07
			$3/2_2^+$	2.80	$5.5 \begin{smallmatrix} + 1.4 \\ - 0.5 \end{smallmatrix}$	5.19 ± 0.08

Table 6.1 (cont.)

				log ft		
J_i^π		J_F^π	E_{xf} (MeV)	ASD1 ^{a)}	EXP ^{b)}	
^{25}Al	$5/2_1^+$	^{25}Mg	$5/2_1^+$	0	3.50 ± 0.03	3.555
			$3/2_1^+$	0.97	6.5	6.27 ± 0.15
			$7/2_1^+$	1.61	4.24 ± 0.05	4.35 ± 0.04
^{26m}Al	0_1^+	^{26}Mg	0_1^+	0	3.49	3.49
^{26}Si	0_1^+	^{26}Al	0_1^+	0.23	3.49	3.49 ± 0.02
			1_1^+	1.06	3.54 ± 0.11	3.53 ± 0.02
			1_2^+	1.85	3.65 ± 0.17	3.81 ± 0.03
			1_3^+	2.07	4.3	4.47 ± 0.10
^{27}Mg	$1/2_1^+$	^{27}Al	$1/2_1^+$	0.84	7.1	4.62 ± 0.02
			$3/2_1^+$	1.01	4.8 ± 0.2	4.94 ± 0.02
^{27}Si	$5/2_1^+$	^{27}Al	$5/2_1^+$	0	3.44 ± 0.02	3.61 ± 0.02
			$3/2_1^+$	1.01	5.8 ± 0.3	7.4 ± 0.2
			$7/2_1^+$	2.21	4.75 ± 0.11	4.76 ± 0.03
			$5/2_2^+$	2.73	5.1 ± 0.4	5.10 ± 0.06
			$3/2_2^+$	2.98	4.22 ± 0.04	4.41 ± 0.04
^{28}Al	3_1^+	^{28}Si	2_1^+	1.78	4.8 ± 0.4	4.87 ± 0.02
^{28}P	3_1^+	^{28}Si	2_1^+	1.78	4.8 ± 0.4	4.85 ± 0.02
			4_1^+	4.62	5.0 ± 0.2	5.82 ± 0.05
			3_1^+	6.28	4.18 ± 0.08	4.78 ± 0.06
			3_2^+	7.80	4.09 ± 0.09	4.76 ± 0.05

a) Calculated with $G_A^2/G_V^2 = 1.29$.

b) Experimental data from ref. 9.

7. Conclusions

The main conclusions of this paper can be summarized as follows.

- i) The correlation assumed to exist between the agreement for the energies on the one hand and the agreement for the transition properties on the other hand is corroborated by the results presented. Thus the results obtained with the ASDI wave functions are in better agreement with experiment than the MSDI results.
- ii) The theoretical errors that were introduced account in a quantitative way for the correlation mentioned sub i).
- iii) When one determines the phenomenological matrix elements of operators in a least-squares fit, one should pay more attention to the weighting factors than is usually done. Thus the dependence of the resulting matrix elements on the set of experimental data taken into account should be considered. As the suppression of particular data is equivalent to the assignment of zero weight, there is an obvious connection with weighting factors. If such a dependence is found one should conclude that the chosen parametrization of the operator is inappropriate. In this paper this situation was encountered, e.g. on considering state-dependent effective charges. Furthermore, the weighting factor should depend also on the reliability of the wave functions. The last point was accounted for in this paper by including the theoretical errors in the weighting factors.
- iv) There is as yet no compelling reason either to use a state-dependent effective charge for the E2 operator or to use renormalized M1 matrix elements for a calculation

in the mass region considered.

- v) If a theoretical error is far too small to explain the difference between the calculated and experimental result, it may be concluded that at least one of the levels involved cannot be described in the given configuration space. In fact, in some cases it was verified explicitly that no linear combination of the calculated wave functions could be found which reproduced the experimental data.
- vi) It was shown that particular combinations of the matrix elements, e.g. mixing ratios, can be quite insensitive to changes in the Hamiltonian. On the other hand certain combinations can be indicated, e.g. branching ratios and lifetimes, that are particularly sensitive to changes in the Hamiltonian. In such cases a good testing ground for the comparison between models is available, provided the experimental data are sufficiently accurate.

References

- 1) Meurders, F., Glaudemans, P.W.M., Van Hienen, J.F.A., Timmer, G.A., Z. Physik A276, 113 (1976)
- 2) Glaudemans, P.W.M., Brussaard, P.J., Wildenthal, B.H., Nucl. Phys. A102 (1967) 593
- 3) Timmer, G.A., Meurders, F., Phys. Lett. 58B (1975) 411
- 4) Barrett, B.R., Kirson, M.W., Phys. Lett. 27B (1968) 544
- 5) Hsu, L.S., Phys. Lett. 25B (1967) 588
- 6) Glaudemans, P.W.M., Endt, P.M., Dieperink, A.E.L., Ann. of Phys. 63 (1971) 134
- 7) Endt, P.M., Van der Leun, C., Nucl. Phys. A235 (1974) 27
- 8) Endt, P.M., Van der Leun, C., Atomic Data and Nuclear Data Tables 13 (1974) 67
- 9) Endt, P.M., Van der Leun, C., Nucl. Phys. A214 (1973) 1
- 10) Schwalm, D. et al., Nucl. Phys. A192 (1972) 449
- 11) Warburton, E.K., Proc. Int. Conf. on nuclear structure and spectroscopy, vol. 2 (Scholars' Press, Amsterdam 1974) p. 506
- 12) Eggenhuisen, H.H. et al., Nucl. Phys. A246 (1975) 231
- 13) Horstman, R.E. et al., Nucl. Phys. A248 (1975) 291
- 14) Eberhardt, J.L., Horstman, R.E., Doubt, H.A., Van Middelkoop, G., Nucl. Phys. A244 (1975) 1
- 15) De Voigt, M.J.A., Glaudemans, P.W.M., De Boer, J., Wildenthal, B.H., Nucl. Phys. A186 (1972) 365
- 16) Rose, H.J., Brink, D.M., Revs. Mod. Phys. 39 (1967) 306
- 17) Wilkinson, D.H., Phys. Rev. C7 (1973) 930
- 18) McGrory, J.B., Phys. Lett. 33B (1970) 327
- 19) Lanford, W.A., Wildenthal, B.H., Phys. Rev. C7 (1973) 668
- 20) Nann, H., Berenson, W., Langford, W.A., Wildenthal, B.H., Phys. Rev. C10 (1974) 1001
- 21) Meyer, M.A., Venter, I., Reitmann, D., Nucl. Phys. A250 (1975) 235
- 22) Ollerhead, R.W., Kean, D.C., Gorman, R.M., Thomson, H.B., Can. J. Phys. 52 (1974) 2329
- 23) De Neys, E.O., Meyer, M.A., Reinecke, J.P.L., Reitmann, D., Nucl. Phys. A230 (1974) 490
- 24) Price, H.G., Twinn, P.J., James, A.N., Sharpey-Schafer, J.F., J. of Phys. A7 (1974) 1151
- 25) Maas, J.W., Utrecht University, private communication

CHAPTER 11

THE USE OF γ -DECAY PROPERTIES FOR THE CONSTRUCTION OF A PHENOMENOLOGICAL SHELL-MODEL HAMILTONIAN

G.A. TIMMER, F. MEURDERS, P.J. BRUSSAARD, P.W.M. GLAUDEMANS
and H.F. DE VRIES

Abstract: Unitary transformations have been applied to shell-model wave functions in the mass region $A = 24 - 28$ in order to fit the experimental γ -decay properties. It is found that usually only small rotations are needed to obtain very good agreement with experiment. Several attempts are described to obtain a Hamiltonian that generates these new wave functions. The results of one approach applied to some levels in ^{28}Si are discussed in more detail. Some extensions of this technique are proposed.

1. Introduction

When one constructs a phenomenological shell-model Hamiltonian, the final results are affected by: i) the choice of the configuration space, ii) the particular parametrization of the Hamiltonian, iii) the choice of the experimental data to which the parameters of the Hamiltonian are fitted and iv) the relative weight that is assigned to the data in the fit.

It is current practice to determine the parameters of such a Hamiltonian from a fit to experimental energies only. The main objective of this paper is to present the results of an

attempt to use experimental information on other observables as well, in particular γ -decay properties.

In a previous paper [1] a Hamiltonian was obtained. This Adjusted Surface Delta Interaction (ASDI) resulted from a fit to the experimental energies of the low-lying positive-parity states in the mass region $A = 24-28$ for a truncated $0d_{5/2}1s_{1/2}0d_{3/2}$ configuration space. In a subsequent paper [2] the γ -decay properties were calculated with the ASDI wave functions. The agreement with experiment was found to be good for strong transitions and of varying quality for weak transitions.

The present approach is motivated by the observation that the γ -decay properties are often very sensitive to small changes in the Hamiltonian. This point was stressed in [2], where this sensitivity was described in terms of a theoretical error. This applies in particular to weak transitions and to the decay properties of closely lying levels with the same (J^π, T) . Hence one can try to find a Hamiltonian which, while differing only slightly from the ASDI Hamiltonian, leads to an improvement over the ASDI results for weak transitions but at the same time does not spoil the agreement obtained for strong transitions. Also the agreement for the energies should be maintained. A recent observation [3] may be of help, i.e. that only a relatively small number of linear combinations of the one- and two-body matrix elements of the Hamiltonian are well determined by a least-squares fit to experimental energies.

The present idea is that, at least initially, the emphasis is shifted from energies to wave functions. In current approaches the wave functions are obtained as a by-product

from a calculation focused on energies. Here we shall start with the construction of wave functions reproducing the experimental γ -decay properties as well as possible in the given configuration space. In sect. 2 a systematic search will be described for the amplitudes of these wave functions in a basis of ASDI wave functions. It is then found that one can obtain a considerable improvement of the γ -decay properties as a result of only minor changes in the original ASDI wave functions.

In sect. 3 methods are discussed which may lead to a Hamiltonian generating the wave functions obtained in sect. 2. Some results will be presented.

Finally, in sect. 4, some of the possible refinements and extensions of the techniques presented will be discussed.

2. The construction of wave functions

Let $\{|\alpha, S_0\rangle\}$ with $\alpha = 1, \dots, M$ denote a given complete set S_0 of orthonormal states in a configuration space of dimension M for given values of A, J^π, T . Suppose that a set of states $\{|\alpha, S_1\rangle\}$ in the same configuration space provides a better description of the γ -decay properties than the set S_0 . We determine the states $|\alpha, S_1\rangle$ by varying the coefficients $a_{\alpha\beta}$ in

$$|\alpha, S_1\rangle = \sum_{\beta=1}^M a_{\alpha\beta} |\beta, S_0\rangle. \quad (2.1)$$

In subsect. 2.1 some arguments are presented leading to a confinement of the space of the parameters $a_{\alpha\beta}$. In subsect. 2.2

the construction of the matrix $a_{\alpha\beta}$ is discussed. For this construction a quantity $Q(a_{\alpha\beta})$ is minimized, defined in subsect. 2.3, which provides an indication for the agreement between the γ -decay properties of the states $|\alpha, S_1\rangle$ with the experimental data. Finally, in subsect. 2.4 some of the results obtained with this procedure are discussed.

2.1 RESTRICTIONS ON $a_{\alpha\beta}$

Two arguments are presented that lead to a substantial reduction of the number of states $|\alpha, S_1\rangle$ to be considered.

The first argument relies on the existence of very strong E2 transitions between low-lying states. Let $|\gamma\rangle$ denote a state providing a good description for the experimentally observed level γ . Suppose that the level γ is fed by a strong E2 transition from another level γ' . The largest possible E2 strength $|\langle\gamma|O(E2)|\gamma'\rangle|^2$ with $O(E2)$ denoting the E2 operator is obtained when the relation $|\gamma'\rangle = PO(E2)|\gamma\rangle$ holds. The operator P projects onto the configuration space available for the description of γ' . When this E2 strength is not larger than the experimental value then it is clear that any serious candidate for the description of γ' should have a large overlap with $|\gamma'\rangle$ as defined above.

The second argument that leads to a reduction of the number of matrices $a_{\alpha\beta}$ to be considered arises from the fact that eventually one would like to obtain a Hamiltonian for which the states $|\alpha, S_1\rangle$, defined in eq. (2.1), are eigenstates. One may try to achieve this by considering only Hamiltonians $H_1 = H_{ASDI} + V$ with V being small. Since then to first order in V the state $|\alpha, S_1\rangle$ is given by

$$|\alpha, S_1\rangle = |\alpha\rangle + \sum_{\beta \neq \alpha} \frac{\langle \beta | V | \alpha \rangle}{E_\alpha - E_\beta} |\beta\rangle \quad (2.2)$$

with $H_{ASDI} |\beta\rangle = E_\beta |\beta\rangle$, it is clear that, provided the energy differences $E_\alpha - E_\beta$ are small, the transformation matrix $a_{\alpha\beta}$ in eq. (2.1) should be close to unity.

In practice only mixtures of the four ASDI states that correspond with the lowest four eigenvalues for each combination A, J^π, T were considered. We are interested mainly in reproducing the γ -decay properties of the lowest two states of each spin. Hence the restriction to the lowest four states ($M=4$) will not noticeably affect the results according to the argument just presented, since the energy differences with higher-lying ASDI states are usually sufficiently large. It may be noted that the same argument was used for the construction of theoretical errors [2].

The two arguments presented in this subsection did not lead to contradictory requirements since the ASDI wave functions already produce very strong E2 transitions for low-lying states. The main practical consequence of the argument concerning strong E2 transitions was that it allowed us to abandon any search for a set of strongly deviating wave functions that may lead to a Hamiltonian that differs substantially from H_{ASDI} . Such wave functions would invalidate the applicability of the first-order perturbational argument.

2.2 THE SEARCH PROCEDURE FOR $a_{\alpha\beta}$

Let $Q(a_{\alpha\beta})$ denote a non-negative quantity measuring the overall agreement between the experimental γ -decay properties and those calculated with the states $|\alpha, S_1\rangle$, defined in

eq. (2.1). This quantity Q , to be discussed in the next subsection, is constructed in such a way that $Q = 0$ indicates perfect agreement. Here it will be described how $a_{\alpha\beta}$ was varied in order to minimize Q .

The general rotation matrix, of which $a_{\alpha\beta}$ provides an example, can be written as the direct product

$$\prod_{\gamma < \delta}^M R_{\gamma\delta}(\phi_{\gamma\delta}), \quad (2.3)$$

where

$$R_{\gamma\delta}(\phi) = \begin{pmatrix} \cos \phi & -\sin \phi \\ \sin \phi & \cos \phi \end{pmatrix} \quad (2.4)$$

is a rotation over an angle ϕ in the plane spanned by the basis vectors $|\gamma, S_0\rangle$ and $|\delta, S_0\rangle$. The rotations considered here are a direct product of rotations in the spaces of each combination J^π, T separately, each of them with dimension $M=4$, as mentioned in the previous subsection.

The search for minimal Q in the space of the parameters $\phi_{\gamma\delta}$ was conducted by the use of the method of steepest descent. Thus one may, and probably will, find a local minimum for Q . This procedure is a compromise between finding the absolute minimum and the requirement that the rotation matrix should be kept close to unity, as discussed in the previous subsection. Successive rotations of the form

$$R_{12}(\phi_{12})R_{23}(\phi_{23})R_{34}(\phi_{34}) \quad (2.5)$$

for one J^π, T combination and unity for the other spin values were employed. One can prove that a repeated application of this transformation for each J^π, T separately is equivalent to the six-parameter transformation given in eq. (2.3) in the space with $M = 4$.

2.3 THE QUANTITY $Q(a_{\alpha\beta})$

Here the quantity Q will be discussed which measures the agreement between theory and experiment.

There are three points to be considered: i) the selection of the calculated observables $\{w_i\}$ that are to be compared with experiment, ii) the functional dependence of Q on $w_i(a_{\alpha\beta})$ and iii) the single-particle matrix elements of the transition operators. The quantities $\{w_i\}$ considered were lifetimes, $E2/M1$ mixing ratios and branching ratios. For the mass region under consideration, i.e. $A = 24-28$, a very large amount of experimental information exists on these quantities, with often very small experimental errors. The experimental data used in the search were taken from [4], supplemented by many recent values that will be included in [5].

For computational convenience it would have been desirable to compare reduced matrix elements instead of the quantities listed above. The main reason for not considering these matrix elements follows from the fact that the errors in the moduli of matrix elements extracted from experiment are in general rather large and, even worse, strongly correlated. It should be mentioned that such a reduction of the experimental data is even impossible when the lifetime or the mixing ratio is unknown. In the present approach, however, the information on branching ratios can always be taken into account. Other

possible candidates for comparison with experiment, like spectroscopic factors, will be considered in the final section of this paper.

The next point to be discussed is the functional dependence of Q on w_i , which is taken as

$$Q = \sum_i \frac{|w_i - w_i^{\text{exp}}|}{|w_i| + |w_i^{\text{exp}}|} g_i, \quad (2.5)$$

where the summation over i covers the lifetimes, branching ratios and mixing ratios that can be compared with experiment. The most satisfactory results have been obtained so far with the weighting factor g_i given by

$$g_i = (5 - m_1^i)(5 - m_2^i) / \Delta^i \quad \text{for } m_1^i, m_2^i \leq 2, \quad (2.6)$$

where m_1^i and m_2^i are the eigenvector numbers of the states involved. States are ordered according to increasing energy such that yrast levels get $m = 1$. For Δ^i either a value 0.1 was used or the relative experimental error, provided the latter is larger than 0.1. The dependence of g_i on the eigenvector numbers reflects the decreasing confidence one should have in the wave functions of higher-lying states. In preliminary calculations it was found that lifetimes were not reproduced well enough. In order to improve the results for the lifetimes it was decided to employ for these quantities twice the weighting factor given in eq. (2.6) with $m_1 = m_2$ the eigenvector number of the decaying state.

The E2 single-particle matrix elements were calculated with harmonic-oscillator wave functions; the size parameter $b = (\hbar/m\omega)^{1/2}$ was determined from the well-known relation $\hbar\omega = 41A^{-1/3}$ MeV. Furthermore an effective isoscalar charge

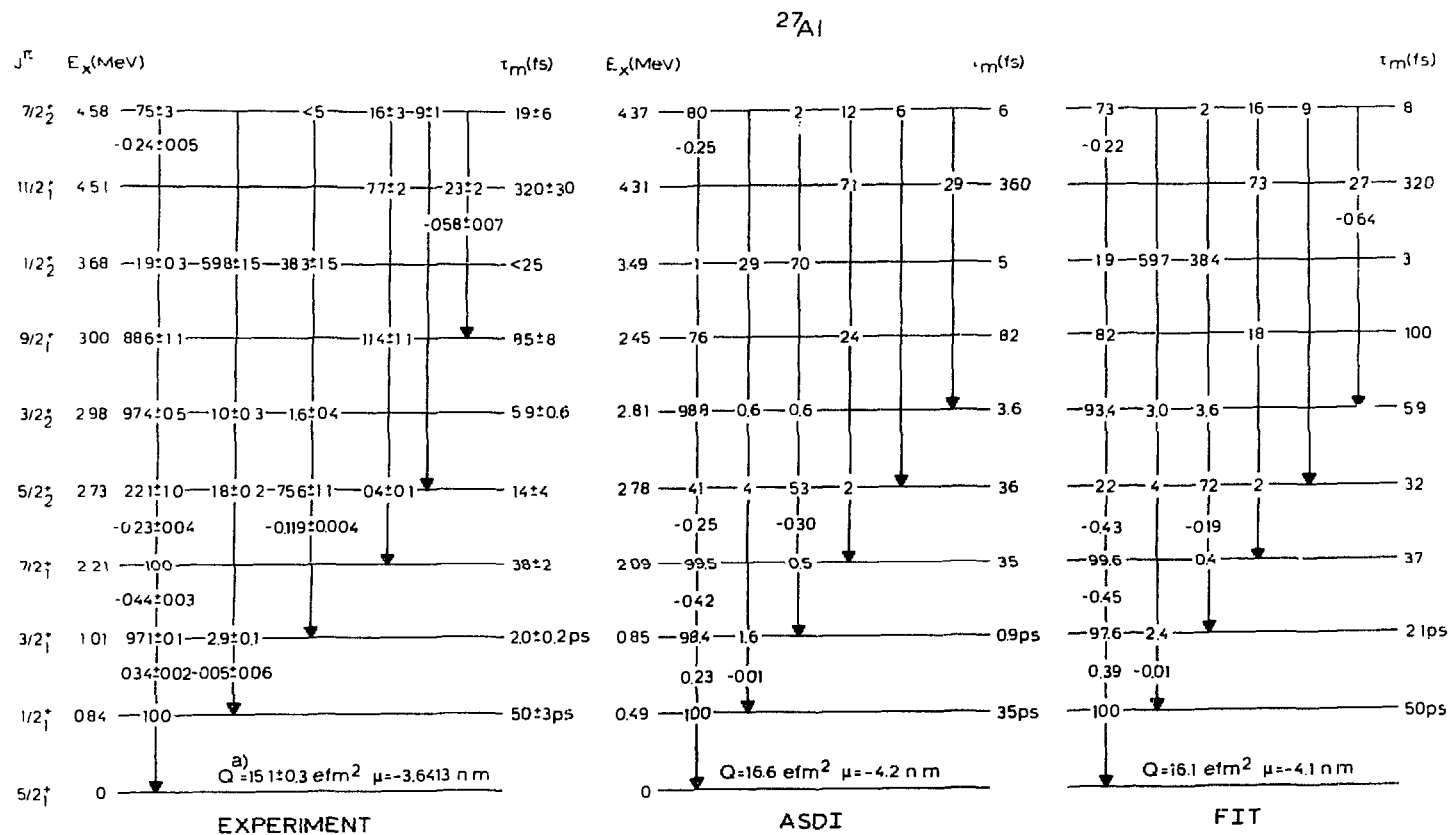


Fig. 2.1. Comparison between the experimental decay scheme of ^{27}Al and the results obtained with ASDI and fitted wave functions.

$e^0 = 2.2e$ was employed. For the M1 single-particle matrix elements bare-nucleon values have been used. The presumably very small admixtures of M3 or E4 radiation have been ignored for the calculation of the decay properties. The energy differences entering the calculation of transition rates were taken from experiment.

2.4 SOME RESULTS

With the technique presented in the previous subsections wave functions were constructed for the low-lying positive-parity states in the mass region $A = 24-28$. The number of steps required to reach a minimum for Q varied between 20 and 100. Mirror nuclei were considered simultaneously. Because of the occurrence of low-lying $T = 1$ states in ^{26}Al , the three nuclei ^{26}Mg , ^{26}Al and ^{26}Si were treated together.

As an example the results obtained for ^{27}Al are displayed in fig. 2.1. One should note the considerable improvement obtained with respect to the ASDI results. In table 2.1 the rotation matrices $a_{\alpha\beta}$ for the ^{27}Al case are shown. It is remarkable that often rather small rotations of the original ASDI wave functions lead to a considerable improvement for the γ -decay properties, especially for branching ratios.

The results obtained for the nuclei not displayed are of comparable quality, although some striking disagreements with experiment remained. It is conceivable that these poor fits are due to an improper truncation of the configuration space.

Table 2.1

The amplitudes of the fitted wave functions of ^{27}Al in an ASDI basis.

J^π	E_x (MeV)	Amplitudes in ASDI basis			
		(1)	(2)	(3)	(4)
$5/2_1^+$	0	0.998	0.062	-0.011	0
$1/2_1^+$	0.84	0.982	0.191	-0.005	-0.005
$3/2_1^+$	1.01	0.997	0.076	0.007	0
$7/2_1^+$	2.21	0.999	-0.054	-0.004	-0.002
$5/2_2^+$	2.73	-0.061	0.920	-0.380	0.066
$3/2_2^+$	2.98	-0.076	0.963	0.259	-0.022
$9/2_1^+$	3.00	0.951	0.239	0.195	0
$1/2_2^+$	3.68	-0.173	0.898	0.009	0.406
$11/2_1^+$	4.51	0.998	-0.070	-0.003	0
$7/2_2^+$	4.58	0.054	0.987	0.120	0.091

3. Construction of a Hamiltonian

The rotated states $|\alpha, S_1\rangle$, obtained in the previous section, are no longer eigenstates of the original Hamiltonian H , except, of course, in the case of exact degeneracy.

Here some attempts will be discussed to construct a Hamiltonian H_1 that in good approximation satisfies the eigenvalue equation $H_1|\alpha, S_1\rangle = E_\alpha^{\text{exp}}|\alpha, S_1\rangle$. An obvious procedure to consider is a fit of H_1 to satisfy the equation

$$\langle \beta, S_1 | H_1 | \alpha, S_1 \rangle = E_\alpha^{\text{exp}} \delta_{\alpha\beta}, \quad (3.1)$$

provided of course that a reasonably complete set of states $|\beta, S_1\rangle$ is available. The use of eq. (3.1) in its general form did not lead to satisfactory results. It turned out to be possible to fit either the diagonal matrix elements or the off-diagonal matrix elements separately, but not simultaneously.

A somewhat more restricted approach that led to rather promising results will now be introduced.

When the ASDI states are employed instead of $|\alpha, S_1\rangle$, eq. (3.1) is solved by construction in good approximation with $H_1 = H_{\text{ASDI}}$. The effects of replacing only a few of the ASDI wave functions were considered. The choice of this subset was restricted by the obvious requirement that the states considered should be orthogonal to the remaining ASDI states. A new Hamiltonian \bar{H} was then determined from a fit of the diagonal matrix elements of eq. (3.1) only. In order to keep the Hamiltonian close to H_{ASDI} the approach discussed in [1] was followed.

As this case was best investigated, the results will be presented that were obtained when the ASDI wave functions for the 2_2^+ and 2_3^+ levels in ^{28}Si at 7.38 and 7.42 MeV, respectively, were replaced by rotated wave functions. The Hamiltonian \bar{H} then obtained indeed differed only slightly from H_{ASDI} , i.e. an average absolute deviation of only 40 keV in the one- and two-body matrix elements was found, whereas the average absolute value is 1.4 MeV. The largest differences of the order of 100 keV occurred for the two-body matrix elements $\langle 1s_{1/2} 0d_{3/2} | \bar{H} | 1s_{1/2} 0d_{3/2} \rangle_{JT}$.

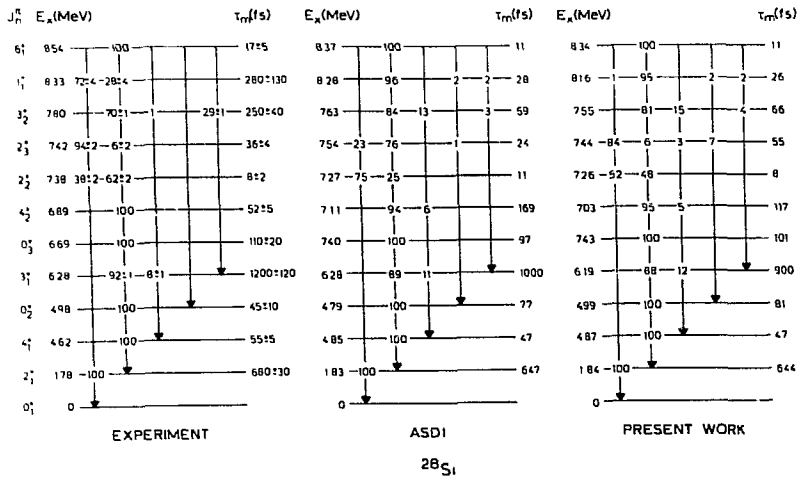


Fig. 3.1. The decay scheme of ^{28}Si .

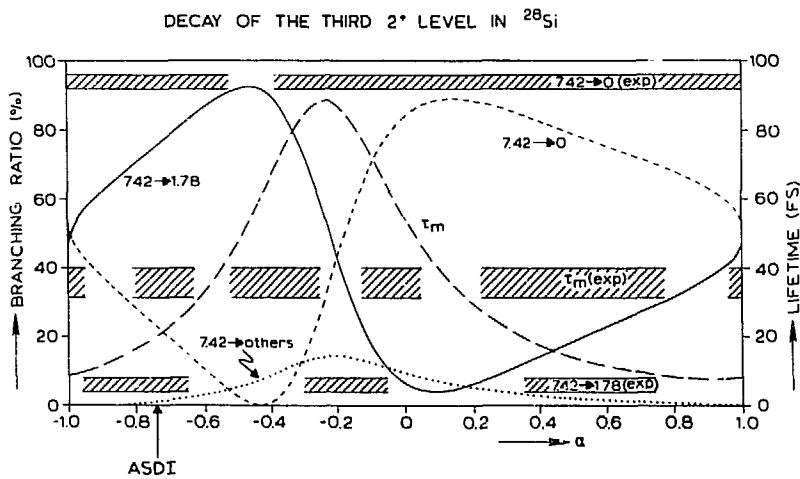


Fig. 3.2. Decay of the 2_3^+ level in ^{28}Si at 7.42 MeV when its wave function is given as $\sqrt{1-\alpha^2} \bar{\psi}_3 - \alpha \bar{\psi}_2$, see text.

Fig. 3.1 displays the decay scheme of ^{28}Si obtained with the eigenfunctions $\bar{\psi}_\alpha$ that resulted from the diagonalization of \bar{H} . One should note the large improvement obtained for the γ -decay properties of the 7.38 and 7.42 MeV levels, whereas the calculated properties of the remaining states are barely affected. From fig. 3.2 one obtains a clear impression of the sensitivity of the γ -decay properties of the $2_{2,3}^+$ levels to changes in the wave functions. In this figure we show the decay properties of the 2_3^+ level as a function of the mixing of the eigenfunctions $\bar{\psi}_2$ and $\bar{\psi}_3$ of the second and third 2^+ levels, respectively. The ASDI wave functions for these levels happen to be very nearly linear combinations of $\bar{\psi}_2$ and $\bar{\psi}_3$. Hence the ASDI results could be indicated in fig. 3.2. All other eigenfunctions of \bar{H} coincided closely with the ASDI wave functions with the exception of the 2_2^+ and 2_3^+ wave functions for $A = 28$, $T = 1$. These levels, however, were neither taken into account in [1] nor in the present fit because of the uncertain spin assignments in the experimental level scheme of ^{28}Al .

4. Discussion

In this section some of the possible refinements and extensions of the techniques presented are discussed.

A first point concerns the effective single-particle transition matrix elements (SPME) that should be used. The SPME used in this calculation resulted, apart from a slight enhancement of the effective isoscalar charge for the E2

operators, from a fit to experimental reduced transition strengths as described in [2]. It seems desirable to fit the SPME directly to quantities like lifetimes, branching ratios and mixing ratios for the same reasons that were mentioned in sect. 2.3. It is clear that such a procedure interferes with the line followed in this paper. In fact one should follow an iterative scheme by fitting in small steps alternately wave functions with given SPME and determine new SPME with the wave functions thus obtained. A possible oscillatory behaviour of the solution of course must be envisaged.

A second remark concerns the choice of the configuration space. In the procedure of section 2 linear combinations of wave functions in a given configuration space were considered. One also may consider the effect of mixing with wave functions outside the initial space. For example, the effect of adding $(Of_{7/2})^2$ components to the $A = 24-28$ wave functions might show up rather strongly in view of the large values of the SPME $\langle Of_{7/2} | Op | Of_{7/2} \rangle$, where Op denotes either the E2 or the M1 operator.

A further remark concerns the experimental data that should be taken into account in the search for good wave functions. The main reason for not considering Gamov-Teller matrix elements is a consequence of the fact that it is probably a shortcoming of the configuration space employed that log ft values are not well described by the ASDI wave functions as discussed in [2]. Spectroscopic factors should certainly be included in searches as described in section 2. In order to get rid of the large experimental errors in individual spectroscopic factors one should for a given ℓ -value consider their ratios.

Other quantities that may be included are electric and magnetic static moments. In view of the rather scanty experimental information they were not yet considered. Very intriguing quantities to consider along these lines are (e, e') form factors. All kinds of interference effects connected with the rotation of wave functions may show up much clearer when one considers the momentum dependence instead of only the photon point. Furthermore form factors allow the consideration of separate E2 and M1 matrix elements, a property they share with static moments.

A last remark concerns the construction of the Hamiltonian. Up to now it turned out to be impossible to construct a Hamiltonian that generates all wave functions desired. There are of course effects from the truncation of the configuration space that frustrate such an endeavour, i.e., as mentioned before, the "true" wave function may have a substantial component outside the configuration space and the underlying assumption that the effective Hamiltonian may be given as a one- and two-body interaction may be erroneous. Nevertheless, a procedure that actually may be considered is a repeated application of the technique presented here, i.e., instead of considering ASDI wave functions as a starting point one may use the wave functions of the Hamiltonian generated here.

References

- 1) Meurders, F., Glaudemans, P.W.M., Van Hienen, J.F.A.,
Timmer, G.A.: Z. Physik A276, 113 (1976)
- 2) Timmer, G.A., Meurders, F., Brussaard, P.J., Van Hienen,
J.F.A.: chapter I of this thesis
- 3) Chung, W., Thesis, Michigan State University, (1976)
- 4) Endt, P.M., Van der Leun, C.: Nucl. Phys. A214, 1 (1973)
- 5) Endt, P.M., Van der Leun, C.: to be published in 1977

CHAPTER III

CALCULATION OF SPURIOUS ADMIXTURES IN SHELL-MODEL WAVE FUNCTIONS

G.A. TIMMER, P.J. BRUSSAARD and G.F. DELEN

Abstract: The expectation value of the square of the centre-of-mass position operator is calculated and used to obtain an estimate for the intensity of spurious centre-of-mass components in shell-model wave functions. The method is applied to some wave functions for negative-parity levels in $A = 32$ nuclei.

1. Introduction

The Hilbert space in which one usually describes the nuclear A -particle system allows $3A$ translational degrees of freedom, whereas the description of the intrinsic motion of the nucleus requires only $3A-3$ translational degrees of freedom. The superfluous degrees of freedom in the description of the intrinsic motion lead to the presence of the spurious states, i.e. states for which the centre-of-mass (CM) is not in its ground state.

Several methods have been devised to cope with the problem of the spurious states. In sect.2 some comments on a few of them will be given. This will lead to the conclusion that at

present there is no satisfactory procedure to treat this problem rigorously. The main part of this chapter is devoted to the presentation of a somewhat more modest approach to the problem of the spurious states. The method presented will provide no way to separate the consequences of CM motion from those of the intrinsic motion for quantities of interest as e.g. transition rates. The only aim is to give a measure for the admixture of spurious states in a given shell-model wave function. In sect.3 expressions for the matrix element of the square of the CM position operator between multishell jj -coupled basis states are derived. In sect.4 it is shown how these matrix elements, on some additional assumptions, can be used to obtain the intensity of the spurious admixture in a given state. The method is applied finally to shell-model wave functions of $A = 32$ nuclei.

2. Other methods

In this section some methods to treat the spurious-state problem will be mentioned.

If one assumes a harmonic-oscillator (h.o.) potential without spin-orbit splitting for the single-particle states, the Hamiltonian can be separated in an intrinsic and a CM part [1]. The latter has again the h.o. form. It was shown by Lee and Baranger [2] how one may then proceed to construct all states with the CM in an excited state, i.e. one constructs the spurious states. This is achieved by introducing an isoscalar vector operator

$$\vec{A}^\dagger = \frac{1}{N} \sum_{k=1}^N \vec{a}^\dagger(k), \quad (2.1)$$

where

$$\vec{a}(k) = \sqrt{\frac{M\omega}{2\hbar}} \vec{r}(k) - \frac{i}{\sqrt{2m\hbar\omega}} \vec{p}(k) \quad (2.1)$$

is the single-particle operator that excites particle k to the next higher oscillator shell (see e.g. ref. [3]).

This approach has been applied in the following way. If P denotes the projection operator onto the spurious states, the operator $(1-P)H(1-P)$ was diagonalized for ^{18}O and ^{18}F in a $(0p_{1/2})^n(0d_{5/2})^{6-n-m}(1s_{1/2})^m$ configuration space. The matrix elements given in [4] were used for the effective Hamiltonian H . The resulting changes in the spectra and transition properties of the wave functions, when compared with the results of diagonalizing H , turned out to be unsatisfactory. The main reason for this failure is to be found in the fact that in this calculation, as in most other calculations, the configuration space is too small to accommodate most spurious states completely. Thus, since model states in a truncated configuration space are the projections of the true states in the complete Hilbert space, one is faced with the serious problem that the two projections involved here - i.e. projecting off the spurious states and projecting onto the truncated model-space - do not commute.

Two other, in principle very promising, approaches to the spurious-state problem should be mentioned. The first approach

is directed towards the explicit construction of translationally invariant wave functions [5]. This, however, requires the introduction of singular operators that do not seem to be very well suited for application in a shell-model calculation. In [6] this approach is criticized from a mathematical point of view.

Finally we would like to mention the approach [7-9] in which one imposes a constraint on the CM motion by adding a h.o. potential of extremely high energy $\hbar\omega_{\text{CM}}$. This method has been criticized recently in [10]. The arguments need not be repeated here.

3. The matrix elements of R^2

In this section expressions will be given for the matrix elements of the operator R^2 , i.e. the square of the position operator of the CM of A particles of equal mass

$$R^2 = \left(\frac{1}{A} \sum_{i=1}^A \vec{r}_i \right)^2. \quad (3.1)$$

In the next section the matrix elements of R^2 will be used to obtain an estimate for spurious content in shell-model wave functions. In the second-quantization formalism this operator reads:

$$R^2 = \frac{1}{A^2} \sum_{\lambda\mu} [\lambda]^{\frac{1}{2}} \langle \lambda | r^2 | \mu \rangle \begin{array}{c} A^\lambda \quad B^\mu \\ \triangle \\ 0 \end{array} +$$

$$- \frac{2}{A^2} \sum_{\substack{\lambda \leq \mu \\ \sigma \leq \tau, \Delta}} [\Delta]^{\frac{1}{2}} W_{\lambda\mu\sigma\tau}^\Delta \zeta_{\lambda\mu} \zeta_{\sigma\tau} \begin{array}{c} A^\mu \quad B^\tau \\ \triangle \quad \triangle \\ 0 \end{array} B^\tau \quad (3.2)$$

The indices λ and μ cover a complete set of single-particle states. A direct product notation is employed; e.g.

$$[\lambda] = [j_\lambda] [t_\lambda] \equiv (2j_\lambda + 1) (2t_\lambda + 1), \quad (3.3)$$

and the fermion creation operator A^λ and time-reversed annihilation operator B^μ are coupled as indicated in the diagrams in both configuration and isospin space. The normalization constants $\zeta_{\lambda\mu}$ are given by

$$\zeta_{\lambda\mu} \equiv (1 + \delta_{\lambda\mu})^{-\frac{1}{2}}. \quad (3.4)$$

Further details on this formalism can be found in [1]. The two-body matrix element $W_{\lambda\mu\sigma\tau}^\Delta$ is given by

$$W_{\lambda\mu\sigma\tau}^\Delta = \langle \lambda\mu; \Delta | \vec{r}_1 \cdot \vec{r}_2 | \sigma\tau; \Delta \rangle. \quad (3.5)$$

The two-particle states in eq.(3.5) are antisymmetric and normalized. The matrix element can be factorized into

$$W_{\lambda\mu\sigma\tau}^{\Delta} = \zeta_{\lambda\mu} \zeta_{\sigma\tau} (-1)^{\mu+\sigma+\Delta} (1-(-1)^{\Delta} P_{\sigma\tau}) \left\{ \begin{matrix} \lambda\mu\Delta \\ \tau\sigma\nu \end{matrix} \right\} \langle \lambda || \vec{r} || \sigma \rangle \langle \mu || \vec{r} || \tau \rangle, \quad (3.6)$$

where $P_{\sigma\tau}$ interchanges the labels σ and τ and the quantity ν assumes the value $\nu = 1$ in configuration space and $\nu = 0$ in isospace.

Many-body matrix elements of the type

$$\langle Z^{\Gamma} | R^2 | Z^{\Gamma'} \rangle \quad (3.7)$$

will be evaluated, where it is assumed that some shell λ_c exists so that the shells $\lambda \leq \lambda_c$ in both the initial and the final state are closed. Furthermore, only those cases are considered where the configuration space is truncated in such a way that the single-particle states $|nljm\rangle$ are uniquely determined by l, j and m , i.e. for each set l, j, m only one value of the radial quantum number n occurs. In virtually all shell-model calculations this restriction is made and therefore no severe limitations are introduced in this way.

After insertion of the right-hand side of eq.(3.2) the matrix element (3.7) can be divided into three parts:

$$\langle R^2 \rangle = \langle S_1 \rangle + \langle S_2 \rangle + \langle S_3 \rangle. \quad (3.8)$$

The operator S_1 stands for the single-particle part of R^2 .

The operators S_2 and S_3 are obtained when the summations in the two-particle terms of eq.(3.2) are written as partial summations over $\lambda \leq \lambda_c$ and $\lambda > \lambda_c$, respectively.

Owing to (i) parity conservation by the operator r^2 , (ii) closure of the core and (iii) the previous assumption concerning the truncation of the configuration space, one can derive the result:

$$Z^\Gamma |S_1| Z^{\Gamma'} \rangle = \frac{1}{A^2} \sum_{\lambda} n_{\lambda} \langle \lambda | r^2 | \lambda \rangle \delta_{\Gamma, \Gamma'}. \quad (3.9)$$

Here n_{λ} represents the number of particles in shell λ .

As the closed shells of the core are coupled to zero spin and isospin, the contribution $\langle S_2 \rangle$ in eq.(3.8) can be reduced to

$$\langle Z^\Gamma | S_2 | Z^{\Gamma'} \rangle = -\frac{2}{A^2} \sum_{\substack{\lambda \leq \lambda_c \\ \mu > \lambda}} n_{\mu} [\mu]^{-1} |\langle \lambda || \vec{r} || \mu \rangle|^2 \delta_{\Gamma, \Gamma'}. \quad (3.10)$$

For future reference the result for $\langle S_1 \rangle + \langle S_2 \rangle$ is quoted in the form

$$\begin{aligned} \langle Z^\Gamma | S_1 + S_2 | Z^{\Gamma'} \rangle = & \left\{ \frac{1}{A^2} \sum_{\lambda \leq \lambda_c} n_{\lambda} \langle \lambda | r^2 | \lambda \rangle - \frac{2}{A^2} \sum_{\lambda < \mu \leq \lambda_c} |\langle \lambda || \vec{r} || \mu \rangle|^2 \right\} \delta_{\Gamma, \Gamma'} + \\ & + \sum_{\lambda_c < \mu} n_{\mu} \left\{ \frac{1}{A^2} \langle \mu | r^2 | \mu \rangle - \frac{2}{A^2} [\mu]^{-1} \sum_{\lambda \leq \lambda_c} |\langle \lambda || \vec{r} || \mu \rangle|^2 \right\} \delta_{\Gamma, \Gamma'}, \end{aligned} \quad (3.11)$$

where use is made of the relation $n_\lambda = [\lambda]$ that holds for a closed shell λ .

A lengthy but straightforward calculation yields for the third contribution to eq.(3.8):

$$\langle S_3 \rangle = \frac{-2}{\sqrt{3}A^2} \sum_{\substack{\lambda_c < \lambda \leq \mu \\ \lambda_c < \sigma < \tau}} \zeta_{\lambda\mu}^2 \zeta_{\sigma\tau}^2 (1 + P_{\sigma\tau}) \langle \lambda || \vec{r} || \sigma \rangle \langle \mu || \vec{r} || \tau \rangle \times$$

$$\langle \begin{array}{c} B^\sigma \quad A^\mu \\ \diagdown \quad \diagup \\ \text{v} \quad \text{v} \\ \diagup \quad \diagdown \\ A^\lambda \quad B^\tau \\ 0 \end{array} \rangle - \frac{2}{A^2} \sum_{\lambda_c < \lambda < \mu} \langle \lambda || \vec{r} || \mu \rangle \langle \mu || \vec{r} || \lambda \rangle (-1)^\Delta \times$$

$$\left[\frac{\Delta}{\lambda\lambda\mu} \right]^{\frac{1}{2}} \langle \begin{array}{c} B^\mu \quad A^\mu \\ \diagdown \quad \diagup \\ \Delta \quad \Delta \\ \diagup \quad \diagdown \\ A^\lambda \quad B^\lambda \\ 0 \end{array} \rangle. \quad (3.12)$$

Again, this equation holds only provided the limitations on the configuration space that were described before are satisfied. Furthermore, in order to obtain the simple restrictions on the summations in eq.(3.12) it was assumed that the coupling order of the active shells is such that all states of one parity π precede all those shells with the opposite parity $-\pi$. For numerical evaluations of $\langle R^2 \rangle$ it is, as far as $\langle S_3 \rangle$ is concerned,

easier to use eq.(3.2) directly, provided one has a computer code for calculating matrix elements of one- and two-body scalar operators at one's disposal, e.g. the Oak Ridge-Rochester code [11]. In such a calculation the terms between the second set of curly braces in eq.(3.11) may be included to play the role of single-particle energies.

4. Spurious content of shell-model states

On the assumption that CM excitations of energy $2\hbar\omega$ (or higher) may be neglected, one can write a shell-model state as

$$\begin{aligned} \Psi_{JM,\gamma}^{\pi}(\vec{r}_1, \dots, \vec{r}_A) = & \alpha \chi_{000}^{+1}(\vec{R}) \phi_{JM,\gamma}^{\pi}(\xi) + \\ & + \sum_{J'm\gamma'} \beta (1mJ'M-m|JM) \chi_{01m}^{-1}(\vec{R}) \phi_{J'M-m,\gamma'}^{-\pi}(\xi). \end{aligned} \quad (4.1)$$

In this expression $\chi_{nlm}^{\pi}(\vec{R})$ represents the h.o. wave function for the CM motion, whereas $\{\phi_{JM,\gamma}^{\pi}(\xi)\}$ denotes a complete set of wave functions depending on the intrinsic coordinates ξ . The explicit dependence [12] of ξ on the laboratory coordinates \vec{r} need not be known.

The expectation value of R^2 in the state defined by eq.(4.1) is given by

$$\langle \Psi_{JM,\gamma}^{\pi} | R^2 | \Psi_{JM,\gamma}^{\pi} \rangle = \frac{3}{2} \frac{b^2}{A} \left(1 + \frac{2}{3} \beta_{\gamma}^2 \right), \quad (4.2)$$

where β_{γ}^2 is defined as

$$\beta_{\gamma}^2 = \sum_{J'\gamma'} \beta_{J'\gamma'}^2, \quad (4.3)$$

and use is made of the relation

$$\langle \chi_{nlm}^{\pi} | R^2 | \chi_{nlm}^{\pi} \rangle = (2n+1+3/2) \frac{b^2}{A}. \quad (4.4)$$

The quantity β_{γ}^2 gives the intensity of the spurious admixture in $\Psi_{JM,\gamma}^{\pi}$. By calculating the left-hand side of eq.(4.2) with the expressions given in sect.3, it is thus possible to obtain β_{γ}^2 for given shell-model wave functions.

The technique described above was applied to some wave functions of negative-parity states in ^{32}P and ^{32}S . These wave functions were obtained [13] in the configuration space $(1s_{1/2}^{-} 0d_{5/2}^{-})^3 (0f_{7/2}^{-} 1p_{3/2}^{-})^1$ employing a modified surface-delta interaction.

The results shown in table 1 indicate the small spurious content of these wave functions. This is not very surprising, though, since with h.o. wave functions all states consisting of a closed ^{16}O core and the other nucleons occupying the $0d$ - $1s$ shell are known to be free of spuriousity [1,2]. The

Table 1

The spurious content β_Y^2 of
some shell-model wave functions from ref.[13]

state γ	β_Y^2	
	32p	32s
$\bar{2}_1$	0.009	0.009
$\bar{2}_2$	0.031	0.017
$\bar{2}_3$	0.017	0.048
$\bar{3}_1$	0.029	0.007
$\bar{3}_2$	0.012	0.042
$\bar{3}_3$	0.018	0.012
$\bar{4}_1$	0.001	0.002
$\bar{4}_2$	0.008	0.020
$\bar{4}_3$	0.007	0.005

The CM excited states are then obtained when the operator given in eq.(2.1) is applied. The excitations that the vector operator \vec{A}^\dagger can produce in a model space with a closed $0d_{5/2}^-$ subshell, are given by $1s_{1/2} \rightarrow 1p_{1/2}, 1p_{3/2}$ and $0d_{3/2} \rightarrow 1p_{1/2}, 1p_{3/2}, 0f_{5/2}$. Since only the $0f_{7/2}$ and the $1p_{3/2}$ subshells are considered in the fp shell, only the components of the wave functions with a particle in the $1p_{3/2}$ orbit will contribute to the spuriousity.

In principle it is of interest to investigate the relation between the amount of spuriousity in a given wave function and the quality of the agreement one obtains on calculating decay properties using the same wave function. It should, however, be mentioned that the E1 transition strengths calculated with the wave functions of [13] gave such poor agreement with experiment that this discrepancy cannot be attributed to spurious states effects only but it arises also from an apparent inadequate model space.

References

- 1) Elliott, J.P.E., Skyrme, T.H.R.: Proc. Roy. Soc. A232, (1955) 561
- 2) Baranger, E., Lee, C.W.: Nucl. Phys. 22, (1961) 157
- 3) Messiah, A.: Quantum Mechanics, North-Holland publ. comp. 1965, vol. I, p. 434
- 4) Zuker, A., Buck, B., McGrory, J.B.: Phys. Rev. Lett. 21, (1968) 39
- 5) Gartenhaus, S., Schwartz, C.: Phys. Rev. 108, (1957) 482
- 6) Palumbo, F.: Phys. Lett. 37B, (1971) 341
- 7) Palumbo, F.: Nucl. Phys. A99, (1967) 100
- 8) Scheid, W., Greiner, W: Ann. of Phys. 48, (1968) 493
- 9) Gloecker, D.H., Lawson, R.D.: Phys. Lett. 53B, (1974) 313
- 10) McGrory, J.B., Wildenthal, B.H.: Phys. Lett. 60B, (1975) 5
- 11) Frenck, J.B., Halbert, E.C., McGrory, J.B., Wong, S.S.N.: in Advances in Nuclear Physics, vol. 3, ed. Baranger, M., Vogt, E. (Plenum Press, New York, 1969)
- 12) Aviles, J.B.: Ann. of Phys. 42, (1967) 403
- 13) Van Hienen, J.F.A.: Thesis Utrecht University, 1975

SAMENVATTING

De in dit proefschrift beschreven berekeningen hebben betrekking op twee verschillende aspecten van het kernspectroscopisch onderzoek. In de eerste twee hoofdstukken worden voornamelijk electromagnetische eigenschappen berekend van kernen in het massagebied $A = 24 - 28$ en wordt ingegaan op mogelijke verbeteringen in bestaande golffuncties. In het derde hoofdstuk besteden we aandacht aan het probleem van de onechte toestanden ('spurious states').

Van elk der hoofdstukken volgt nu een korte samenvatting. *Hoofdstuk I.* Hierin worden elektrische quadrupool- en magnetische dipoolmatrizelementen berekend met twee stelsels golffuncties die bij respectievelijk de 'modified surface-delta interaction' (MSDI) en de 'adjusted surface-delta interaction' (ASDI) behoren. Het blijkt dat de ASDI-golffuncties een betere beschrijving van de experimentele eigenschappen geven dan de MSDI-golffuncties.

De één-deeltjes matrizelementen van de overgangsoperatoren worden bepaald door een aanpassing aan experimentele overgangsterkten en statische momenten. Het blijkt dat volstaan kan worden met een toestandsonafhankelijke effectieve lading en een ongerenormeerde magnetische dipooloperator.

In dit eerste hoofdstuk wordt verder het begrip *theoretische fout* geïntroduceerd. Deze theoretische fouten geven een aanwijzing omtrent de gevoeligheid van berekende electromagnetische eigenschappen voor veranderingen in de Hamiltoniaan. Het blijkt dat deze fouten in het algemeen de verschillen tussen experiment en theorie verklaren.

Tenslotte worden met behulp van de ASDI-golffuncties voorspellingen gegeven voor statische momenten en worden log ft

waarden berekend voor toegestaan beta-verval.

Hoofdstuk II. Reeds in het eerste hoofdstuk wordt in sommige gevallen expliciet aangegeven hoe lineaire combinaties van ASDI-golffuncties tot een betere beschrijving van de experimentele vervalseigenschappen kunnen leiden dan met de oorspronkelijke golffuncties mogelijk is. In dit hoofdstuk wordt dit effect op een meer systematische wijze onderzocht. Het blijkt dat in het massagebied $A = 24-28$ golffuncties gevonden kunnen worden die, hoewel slechts weinig afwijkend van de ASDI-golffuncties, tot een grote verbetering van de berekende eigenschappen van gammaverval leiden. In het laatste deel van het tweede hoofdstuk worden enige pogingen beschreven om een Hamiltoniaan te vinden die deze nieuwe golffuncties als eigenfuncties voortbrengt. Voor enige gevallen in ^{28}Si is dat inderdaad gelukt.

Hoofdstuk III. In dit hoofdstuk worden formules afgeleid voor de berekening van de verwachtingswaarde van het kwadraat van de zwaartepuntscoördinaat. Vervolgens wordt aangetoond hoe deze verwachtingswaarden gebruikt kunnen worden om de intensiteit van onechte toestanden in schillenmodelgolffuncties te berekenen. De methode wordt toegepast op enige reeds uit de literatuur beschikbare golffuncties in ^{32}P en ^{32}S .

CURRICULUM VITAE

Na zijn middelbare schooltijd aan het Erasmiaans Gymnasium (Gymnasium β) in Rotterdam, begon de schrijver van dit proefschrift in 1961 met de studie in de wis- en natuurkunde aan de Rijksuniversiteit te Leiden. Het kandidaatsexamen werd in 1965 behaald. Vervolgens werd als hoofdrichting theoretische natuurkunde gekozen, waarin in 1968 het doctoraal examen werd afgelegd, met als bijvakken onderwerpen uit de wiskunde.

Van 1969 af is de schrijver werkzaam bij de Utrechtse werkgroep theoretische kernfysica als wetenschappelijk medewerker van de Stichting Fundamenteel Onderzoek der Materie. De eerste jaren van het onderzoek werden voornamelijk besteed aan de opbouw van computerprogrammatuur ten behoeve van schillenmodelberekeningen. Op uitnodiging van de universiteit van Liverpool werden in 1974 ook daar de programma's geïmplementeerd. Door de Stichting voor Fundamenteel Onderzoek der Materie werd hij in de gelegenheid gesteld om in 1971 een winterschool in Triëst te bezoeken en om in 1972-1973 verscheidene malen in Liverpool te werken.

